



Transcriptional programs mediating neuronal toxicity and altered glial-neuronal signaling in a *Drosophila* knock-in tauopathy model

Hassan Bukhari, Vanitha Nithianadam, Rachel A. Battaglia, et al.

Genome Res. published online April 10, 2024

Access the most recent version at doi:[10.1101/gr.278576.123](https://doi.org/10.1101/gr.278576.123)

P<P	Published online April 10, 2024 in advance of the print journal.
Accepted Manuscript	Peer-reviewed and accepted for publication but not copyedited or typeset; accepted manuscript is likely to differ from the final, published version.
Open Access	Freely available online through the <i>Genome Research</i> Open Access option.
Creative Commons License	This manuscript is Open Access. This article, published in <i>Genome Research</i> , is available under a Creative Commons License (Attribution 4.0 International license), as described at http://creativecommons.org/licenses/by/4.0/ .
Email Alerting Service	Receive free email alerts when new articles cite this article - sign up in the box at the top right corner of the article or click here .

Advance online articles have been peer reviewed and accepted for publication but have not yet appeared in the paper journal (edited, typeset versions may be posted when available prior to final publication). Advance online articles are citable and establish publication priority; they are indexed by PubMed from initial publication. Citations to Advance online articles must include the digital object identifier (DOIs) and date of initial publication.

To subscribe to *Genome Research* go to:
<https://genome.cshlp.org/subscriptions>

Published by Cold Spring Harbor Laboratory Press

Transcriptional programs mediating neuronal toxicity and altered glial-neuronal signaling in a *Drosophila* knock-in tauopathy model

Running title: *Drosophila* knock-in tauopathy model

Hassan Bukhari,^{1,2} Vanitha Nithianandam,^{1,2} Rachel A. Battaglia,^{1,2} Anthony Cicalo,^{2,3,4}
Souvarish Sarkar,¹ Aram Comjean,⁵ Yanhui Hu,⁵ Matthew J. Leventhal,^{6,7} Xianjun Dong,^{2,3,4} and
Mel B. Feany^{1,2*}

¹Department of Pathology, Brigham and Women's Hospital, Harvard Medical School, Boston, Massachusetts 02115

² Aligning Science Across Parkinson's (ASAP) Collaborative Research Network, Chevy Chase, MD 20815

³Genomics and Bioinformatics Hub, Brigham and Women's Hospital, Boston, MA 02115

⁴Department of Neurology, Brigham and Women's Hospital, Harvard Medical School, Boston, MA, 02115

⁵Department of Genetics, Blavatnik Institute, Harvard Medical School, Boston, MA 02115

⁶Department of Biological Engineering, Massachusetts Institute of Technology, Cambridge, MA 02139

⁷MIT Ph.D. Program in Computational and Systems Biology, Cambridge, MA 02139

*Correspondence should be addressed to:

Mel B. Feany, M.D., Ph.D.

Department of Pathology

Brigham and Women's Hospital,

Harvard Medical School

77 Ave Louis Pasteur, Room 630F

Boston, MA 02115

Phone: 617-525-4405

Fax: 617-525-4422

Email: mel_feany@hms.harvard.edu

1 **Abstract**

2 Missense mutations in the gene encoding the microtubule-associated protein tau cause
3 autosomal dominant forms of frontotemporal dementia. Multiple models of frontotemporal
4 dementia based on transgenic expression of human tau in experimental model organisms,
5 including *Drosophila*, have been described. These models replicate key features of the human
6 disease, but do not faithfully recreate the genetic context of the human disorder. Here we use
7 CRISPR-Cas mediated gene editing to model frontotemporal dementia caused by the tau
8 P301L mutation by creating the orthologous mutation, P251L, in the endogenous *Drosophila tau*
9 gene. Flies heterozygous or homozygous for tau P251L display age-dependent
10 neurodegeneration, metabolic defects and accumulate DNA damage in affected neurons. To
11 understand the molecular events promoting neuronal dysfunction and death in knock-in flies we
12 performed single-cell RNA sequencing on approximately 130,000 cells from brains of tau P251L
13 mutant and control flies. We found that expression of disease-associated mutant tau altered
14 gene expression cell autonomously in all neuronal cell types identified. Gene expression was
15 also altered in glial cells, suggestive of non-cell autonomous regulation. Cell signaling pathways,
16 including glial-neuronal signaling, were broadly dysregulated as were brain region and cell-type
17 specific protein interaction networks and gene regulatory programs. In summary, we present
18 here a genetic model of tauopathy, which faithfully recapitulates the genetic context and
19 phenotypic features of the human disease and use the results of comprehensive single cell
20 sequencing analysis to outline pathways of neurotoxicity and highlight the potential role of non-
21 cell autonomous changes in glia.

22

23 **Introduction**

24 The neuronal microtubule-associated protein tau forms insoluble deposits termed neurofibrillary
25 tangles and neuritic threads in neuronal soma and processes in a diverse group of age-
26 dependent neurodegenerative diseases, including Alzheimer's disease and frontotemporal
27 dementia. These disorders have collectively been termed "tauopathies" (Feany and Dickson
28 1996; Götz et al. 2019; Goedert 2004). While wild type tau is deposited in Alzheimer's disease
29 and other more common tauopathies, missense mutations in tau occur in rarer familial forms of
30 tauopathy causing neurodegeneration and insoluble tau deposition. Autosomal dominant
31 disease-causing mutations occur throughout the tau protein but are particularly frequent in exon
32 10, which contains one of four microtubule binding repeats (Ghetti et al. 2015). These repeats
33 mediate microtubule (Lee et al. 1989; Butner and Kirschner 1991) and actin (Cabrales Fontela
34 et al. 2017) binding, and are important determinants of tau aggregation (von Bergen et al.
35 2000). Experimental models of tauopathy have been created in diverse model organisms, from
36 yeast to non-human primates, by expressing wild type or frontotemporal dementia-associated
37 mutant forms of human tau in transgenic animals. Mutant forms of tau are typically more toxic
38 than wild type tau in transgenic model organisms. Work in these models has implicated a
39 number of cellular pathways in mediating tau neurotoxicity, including mitochondrial dysfunction
40 (Rhein et al. 2009; DuBoff et al. 2012), oxidative stress (Dias-Santagata et al. 2007; Dumont et
41 al. 2011) and aberrant cell cycle reentry of postmitotic neurons (Khurana et al. 2006; Andorfer et
42 al. 2005).

43 However, while transgenic models have been useful, they do not faithfully replicate the
44 genetic underpinnings of the authentic human disorders and thus may not allow the
45 identification and study of the full complement of important mediators of tauopathy
46 pathogenesis. We have therefore used CRISPR-Cas9 gene editing to model familial
47 frontotemporal dementia caused by missense mutations in tau more precisely in *Drosophila*.
48 Mutation of proline 301 to leucine in exon 10 is the most common mutation of tau in

49 frontotemporal dementia patients (Poorkaj et al. 2001), and has been frequently modeled in
50 transgenic animals (Goedert and Jakes 2005). The overall structure and expression of tau is
51 conserved from mammals to *Drosophila* (Heidary and Fortini 2001), with proline 251 being
52 orthologous to human proline 301. We have therefore replaced *Drosophila* tau proline 251 with
53 leucine (P251L) and phenotypically analyzed the resultant homozygous and heterozygous
54 animals with age. We have additionally performed single-cell sequencing to identify cell
55 populations, networks and signaling systems altered by mutant tau expression.

56

57 **Results:**

58 **Phenotypic analysis of a *Drosophila* knock-in model of frontotemporal dementia**

59 We used CRISPR-Cas9 gene editing to recapitulate the genetic basis of human frontotemporal
60 dementia in the powerful genetic experimental organism *Drosophila* by modeling the disease-
61 causing proline 301 to leucine in fly tau. Protein sequence alignment shows that the
62 microtubule-binding domains, including human tau proline 301 are evolutionary conserved from
63 *Drosophila* to humans (Supplemental Fig. S1). The homologous residue of the human tau
64 proline 301, *Drosophila* tau proline 251, was mutated to leucine using a highly efficient guide
65 RNA along with single-stranded oligodeoxynucleotides (Fig. 1A,B). Mutant tau was expressed at
66 equivalent levels to wild type tau (Supplemental Fig. 2A).

67 Expression of frontotemporal dementia-linked forms of mutant tau, including P301L, lead
68 to age-dependent neuronal loss in patients and in transgenic models (Ghetti et al. 2015; Lewis
69 et al. 2001; Yoshiyama et al. 2007; Götz et al. 2001). We thus examined the histology of brains
70 of heterozygous (P251L / +) and homozygous (P251L) tau knock-in animals with age. We found
71 increased numbers of cortical and neuropil vacuoles in knock-in animals (Fig. 1C,D).
72 Neurodegeneration in *Drosophila* is frequently accompanied by the formation of brain vacuoles

73 (Buchanan and Benzer 1993; Wittmann et al. 2001; Ordonez et al. 2018; Heisenberg and Böhl
74 1979). Increasing numbers of vacuoles were observed with advancing age, and with two copies
75 of the P251L compared with one copy (Fig. 1C,D). Inappropriate neuronal cycle reentry is a
76 feature of human tauopathy (Husseman et al. 2000) and human tau transgenic animals
77 (Andorfer et al. 2005; Khurana et al. 2006). We stained control and tau P251L knock-in brains
78 with an antibody directed to proliferating cell nuclear antigen (PCNA) to assess cell cycle
79 activation (Khurana et al. 2006). We observed increasing cell cycle reentry with age in tau
80 P251L knock-in brains, with more cell cycle activation in homozygotes compared to
81 heterozygotes (Fig. 1E, Supplemental Fig. 2B).

82 Metabolic alterations and mitochondrial dysfunction are pervasive features of
83 neurodegenerative diseases, including tauopathies (DuBoff et al. 2013; Götz et al. 2019). We
84 thus performed metabolic analysis on intact whole fly brains using the Seahorse XFe96
85 Analyzer (Neville et al. 2018). We observed reduced basal oxygen consumption rate (OCR) and
86 a shift in mitochondrial bioenergetics to quiescent metabolic state in tau 251L knock-in animals,
87 with homozygotes showing more impairment than heterozygotes (Fig. 2A,B).

88 Oxidative stress accompanying mitochondrial dysfunction results in damage to key
89 cellular substrates, including DNA. DNA damage commonly occurs in age-related
90 neurodegenerative diseases (Welch and Tsai 2022), including tauopathies (Khurana et al. 2012;
91 Thadathil et al. 2021; Shanbhag et al. 2019). We took two approaches to examining DNA
92 damage in tau P251L knock-in animals. First, we used the comet assay, in which DNA single- or
93 double-strand breaks are demonstrated using single-cell gel electrophoresis (Khurana et al.
94 2012; Frost et al. 2014). We observed that nuclei from brains of tau P251L knock-in flies
95 displayed almost 2-fold longer comet tails than controls (Fig. 2C, arrowheads, D).

96 As a second measure of DNA damage, we immunostained for the histone variant H2Av
97 phosphorylated at serine 137 (pH2Av), a marker of DNA double-strand breaks (Madigan et al.
98 2002; Khurana et al. 2012; Frost et al. 2014). We found significantly increased numbers of
99 double-strand breaks within neurons (Fig. 2E, arrows, arrowheads, F,G). DNA double-strand
100 breaks were elevated with age and in homozygous compared to heterozygous tau P251L
101 knock-in flies (Fig. 2E,F,G). Increased DNA damage was assessed by counting both the
102 numbers of Kenyon cell nuclei containing pH2Av foci, and the number of Kenyon cell nuclei
103 containing more than 2 foci (Fig. 2E, arrows, G), which correlates with increased numbers of
104 DNA double-strand breaks (Lapytsko et al. 2015; Hong and Choi 2013).

105

106 **Single-cell RNA sequencing reveals gene expression changes mediated by pathologic** 107 **tau**

108 Our tau P251L knock-in flies replicate important features of human tauopathies and transgenic
109 models of the disorders. We therefore performed single-cell RNA sequencing to investigate
110 transcriptional programs and cellular pathways altered by expression of mutant tau. Using an
111 optimized brain dissociation method, 10x library preparation, sequencing, and a bioinformatics
112 analysis pipeline, we implemented single-cell RNA sequencing on tau P251L knock-in and
113 control *Drosophila* brains at 10 days of age (Fig. 3A). The 10-day time point was chosen to
114 identify early perturbations related to neuronal dysfunction and degeneration (Fig. 1,2). After
115 stringent quality control 130,489 high-quality cells were retained in the final integrated dataset
116 and 29 clusters of cells were identified. We annotated 26 clusters using a published fly cell atlas
117 (Li et al. 2022). We used the most highly expressed marker genes within each cluster to identify
118 clusters. For instance, we used *dac*, *crb* and *jdp* to annotate Kenyon cells; *Yp1*, *Yp2* and *Yp3* for
119 mushroom body output neurons (MBON); *Mtna*, *CG8369* and *CG1552* for glia; *CG34355*, *Gad1*

120 and *mamo* for medullary neurons; *acj6*, *Li1* and *sosie* for T neurons (Supplemental Figs.
121 S3,S4,S5). The clustered dot plot illustrates enrichment of marker genes in annotated neuronal
122 and glial clusters (Fig. 3C, Supplemental Fig. S4C). Based on prior published analyses (Li et al.
123 2022; Croset et al. 2018; Davie et al. 2018) we further outlined major groups of cells, including
124 Kenyon cells, medullary neurons, mushroom body output neurons (MBON), astrocytes and
125 perineurial glia (Fig. 3B; Supplemental Fig. S3; Supplemental Table S1). As previously
126 observed (Davie et al. 2018), cholinergic neurons were the most common neuronal type defined
127 by neurotransmitter phenotype, followed by GABAergic and glutamatergic neurons
128 (Supplemental Fig. S3). Less abundant clusters of dopaminergic neurons were also identified
129 (Supplemental Fig. S3). In summary, our scRNA sequencing in a precisely edited *Drosophila*
130 tauopathy model, yielded 130,489 high quality cells, and identified cellular populations
131 throughout diverse brain regions and cell types, including rarer cell populations such as
132 astrocytes and perineurial glia.

133 After sample integration, quality control and cluster annotation, we performed differential
134 gene expression analysis (DEG) to identify genes modulated by precise pathologic mutation
135 modeling of tauopathy in the *Drosophila* brain. DEG analysis of all the 26 annotated clusters
136 revealed that tau P251L knock-in altered genes throughout the *Drosophila* brain, in both
137 neurons and glia (Fig. 4A, Supplemental Table S2). We found that 472 genes were up-regulated
138 across all clusters in tau P251L knock-in brains, while 1145 genes were down-regulated
139 (Supplemental Table S3). Transposable elements (*FBti0020120 RR48373-transposable-*
140 *element*, *FBti0063007*, *FBti0019000*, *FBti0019150*, *RR50423-transposable-element*,
141 *FBti0019148*) were frequently up-regulated in P251L knock-in brains (Fig. 4B), consistent with
142 findings from *Drosophila* human tau overexpression models and human Alzheimer's disease
143 brain tissue (Sun et al. 2018; Guo et al. 2018). The set of commonly down-regulated genes was
144 notable for multiple ribosomal protein genes (Fig. 4C), suggesting a translational defect in

145 tauopathy. Multiple nuclear and mitochondrially encoded respiratory chain subunits and other
146 mitochondrial proteins were notably present in the commonly up-regulated and down-regulated
147 gene, as were genes encoding cytoskeletal and associated proteins (*Arc1*, *Msp300*, *Ank2*, *unc-*
148 *104*, *Amph*, *brp*, *alphaTub84B*). Both categories of genes fit well with known mediators of
149 tauopathy pathogenesis (DuBoff et al. 2013; Schulz et al. 2023).

150 As expected, gene enrichment analyses (Fig. 4D; Supplemental Fig. S6) highlighted
151 mitochondrial and cytoskeletal processes. In addition, diverse metabolic and neuronal function
152 pathways, including associated learning, previously associated with Alzheimer's disease and
153 related tauopathies emerged from Gene Ontology (GO) enrichment analyses. Enrichment
154 analysis for human disease associated genes revealed predominantly neurodegenerative
155 disorders, including tauopathy (Fig. 4E).

156

157 **Distinct and shared region- and cell-specific transcriptional programs in tau P251L** 158 **knock-in brains**

159 Significant anatomic and cell type selectivity characterizes human neurodegenerative diseases,
160 including tauopathies. We therefore analyzed gene expression changes separately in
161 anatomically and functionally related groups of cells including the central body (Kenyon cells,
162 MBON and Pox neurons), optic lobe (lamina, medulla, and lobula neurons) and glia (astrocytes
163 and perineurial glia). Volcano plots in Supplemental Fig. 7A, C and F present up-regulated and
164 down-regulated genes in each group of cells. Transposable element were top up-regulated
165 genes in each of the three groups. GO enrichment analyses (Supplemental Fig. 7B,D) identified
166 distinct biological processes altered by mutant tau expression in the central body compared to
167 the optic lobe. Both associative learning and cAMP metabolic process were specifically
168 identified in the central body, correlating with the importance of Kenyon cells in learning and

169 memory in flies and with the central role for cAMP underlying learning and memory (Güven-
170 Ozkan and Davis 2014; Feany and Quinn 1995). Heterochromatin organization and DNA repair,
171 both processes strongly implicated in tauopathy pathogenesis (Fig. 2) (Khurana et al. 2012;
172 Frost et al. 2014; Welch and Tsai 2022) emerged as enriched processes following analysis of
173 the central body and optic lobe separately (Supplemental Fig. 7D). Direct comparison of
174 differentially regulated genes in central body compared to optic lobe neurons revealed 239
175 commonly regulated genes and 562 distinct genes (Supplemental Fig. 7E). Consistent with
176 analysis of the total transcriptome (Fig. 4), shared biological processes included down-
177 regulation of mitochondrial genes and up-regulation of axon guidance-associated genes
178 (Supplemental Fig. 6E; Supplemental Table S4).

179 Since tau is a predominantly neuronal gene (Heidary and Fortini 2001; Goedert 2004;
180 Götz et al. 2019) the observed changes in neuronal transcriptomes may reflect cell-autonomous
181 effects of frontotemporal dementia associated mutant tau protein. Our single-cell approach also
182 revealed significant changes in gene expression in glial cells in tau P251L knock-in brains
183 (Supplemental Fig. 7F,G). Expression of mutant tau may thus exert non-cell autonomous control
184 on glial transcriptional programs. Metabolic processes (Supplemental Fig. 7G) were down-
185 regulated in glia in response to neuronal expression of mutant tau, consistent with the
186 importance of glial metabolism in supporting a wide array of neuronal functions (Nedergaard
187 and Verkhratsky 2012; Verkhratsky et al. 2012). The top two GO processes identified by
188 analysis of up-regulated glial genes were associative learning and regulation of neuronal
189 remodeling, suggesting that coordinate changes in neurons and glia may lead to impairment of
190 critical neuronal functions when mutant tau is expressed by neurons.

191 We next constructed protein interaction networks to explore further the biological
192 pathways altered in tau P251L knock-in brains compared to controls. We used the solution of
193 the prize-collecting Steiner forest algorithm (Tuncbag et al. 2013) to map differentially

194 expressed genes onto a network of physical protein interactions using *Drosophila* interactome
195 data. Networks constructed from the central body, optic lobe and glial cells were substantially
196 distinct (Fig. 5), consistent with differential effects of mutant tau on different anatomic regions
197 and cell types. The electron transport chain was identified in subnetworks from both the optic
198 lobe and glia raising the possibility that mutant tau can influence mitochondrial function in both a
199 cell-autonomous and non-cell autonomous fashion (Figs. 2,5). Regulation of nuclear function
200 was commonly identified in both central body and optic lobe neurons, consistent with a strong
201 influence of neuronally expressed tau on chromatin structure mediated through the Linker of
202 Nucleoskeleton and Cytoskeleton (LINC) complex (Frost et al. 2014, 2016).

203 Protein catabolism was a subnetwork in both central body and glial networks. Protein
204 catabolism was connected to multiple other subnetworks in the central body network and
205 contained multiple proteins previously implicated in Alzheimer's disease, including Appl (fly
206 ortholog of APP), beta-site APP-cleaving enzyme (Bace, a fly homolog of BACE1), three
207 members of the cathepsin family (CtsB1, cathD, CtsF/CG12163), and tau itself identified as a
208 computational network-inferred node. As expected from Gene Ontology analysis (Supplemental
209 Fig. 7G), multiple metabolic subnetworks were identified in the glial network, consistent with the
210 role of glia in providing metabolic support to neurons (Nedergaard and Verkhratsky 2012;
211 Verkhratsky et al. 2012). A subnetwork enriched for nodes associated with fatty acid metabolism
212 was identified in the glial network (Fig. 5), correlating with the important role of glia in lipid
213 metabolism and signaling in both flies and mammalian systems (Goodman and Bellen 2022;
214 Lee et al. 2021). Detailed protein interaction networks identified in the central body, optic lobe
215 and glia are shown in Supplemental Fig. S8-S10.

216

217 **Cell-cell communication and pseudotime trajectory analyses highlight the role of glial**
218 **cells in tau P251L knock-in brains**

219 Altered gene expression (Supplemental Fig. 7) and protein interaction networks (Fig. 5) in glia
220 driven by neuronal-predominant expression of P251L mutant tau suggests perturbed
221 intercellular communication in P251L knock-in brains. We therefore calculated the interaction
222 scores for 196 manually curated ligand-receptor pairs using the FlyPhoneDB quantification
223 algorithm (Liu et al. 2022) in tau P251L knock-in brains and controls. We found significant
224 alterations predicted in major cellular signaling pathways (Fig. 6; Supplemental Fig. S11).
225 Altered signaling is indicated in circle plots in Fig. 6 (A,C,E,G) by nodes representing a unique
226 cell types and edges representing a communication event. The thickness of an edge reflects the
227 interaction strength of the communication event. Dot plots in Fig. 6 (B,D,F,H) display the
228 calculated score of selected ligand-receptor pairs from one cell type to another with the shading
229 of the dot indicating the interaction score and the size of the dot the P value. Many of predicted
230 signaling changes support altered communication between glia and neurons. For instance,
231 synaptic plasticity signaling, assessed by expression of the ligand *spatzle* and *kekkon* receptors,
232 was mainly driven by perineurial glia in the control brain. However, perineurial glial cells in tau
233 P251L knock-in animals had reduced expression of the ligand *spatzle* 5 while recipient cells
234 down-regulated *kekkon* receptors (Fig. 6B). Similarly, expression of the JAK-STAT ligand *upd2*
235 was significantly down-regulated in perineurial glia in tau P251L knock-in brains compared to
236 controls, while the receptor *dome* was reduced in expression in widespread target neuronal
237 clusters (Fig. 6D). There was a predicted up-regulation of JAK-STAT signaling from mushroom
238 body output neurons to a restricted set of neuronal clusters in brains of flies expressing P251L
239 mutant tau (Fig. 6C). In contrast, predicted hippo signaling from mushroom body output neurons
240 to perineurial glial based on decreased levels of the ligand *ds* and receptor *fat* was decreased in
241 tau P251L knock-in brains compared to controls (Fig. 6E).

242 Astrocytic signaling also showed predicted changes in tau P251L knock-in brains
243 compared to controls. JAK-STAT signaling perineurial glia to astrocytes was reduced in mutant
244 tau expressing brains (Fig. 6C), while hippo signaling from astrocytes to multiple neuronal
245 subtypes was increased in tau P251L knock-in brains (Fig. 6E,F). TNF- α signaling from
246 astrocytes was also increased in flies expressing mutant tau, as suggested by increased levels
247 of the ligand eiger and receptor wengen (Fig. 6G,H). Altered astrocyte integrin, hedgehog and
248 insulin signaling was also suggested by changes in expression of ligand and cognate receptor
249 pairs (Supplemental Fig. S11A,D,E).

250 Given altered gene expression (Fig. 4, Supplemental Fig. 7), protein interaction networks
251 (Fig. 5) and predicted signaling (Fig. 6) in glia we next examined gene expression profiles in
252 these non-neuronal cells in more detail (Fig. 7). Transposable elements were significantly up-
253 regulated in both types of glia (Fig. 7A,C; Supplemental Table S5), although one transposable
254 element was highly down-regulated in both glia subsets (*RR48361*). Gene Ontology enrichment
255 analysis highlighted different metabolic pathways in the two cell types. Amino acid and
256 glutamate metabolism pathways were enriched in perineurial glia while L-cysteine, acyl-CoA
257 and cAMP metabolic pathways were enriched in astrocytes (Fig 7B, D).

258 Since we observed significant alterations in glial signaling in tau P251L knock-in brains
259 (Fig. 6; Supplemental Fig. S11) we investigated glial gene trajectories in our single-cell RNA
260 sequencing, focusing on astrocytes because we obtained a large number (nearly 5800) of these
261 cells (Supplemental Table S1). We first subclustered astrocytes into 4 groups (Fig. 7E). We then
262 calculated the entropy of these clusters (Guo et al. 2017) and used cluster 1, which showed the
263 highest entropy (Fig. 7F), as the root for trajectory analysis (Street et al. 2018). A single lineage
264 starting from cluster 1 and progressing sequentially from cluster 2 through cluster 3 and finally
265 to cluster 0 emerged (Fig. 7G). We then clustered differentially expressed genes along the
266 calculated trajectory as presented in the heat map, in which pseudotime is represented in

267 columns from left to right (Fig. 7H). Our pseudotemporal analysis suggests different stages of
268 astrocytic response to tauopathy.

269 Gene Ontology analysis across pseudotime revealed multiple genes involved in
270 signaling pathways (*FMRFa*, *NimB5*), particularly in cholinergic signaling (nicotinic acetylcholine
271 receptor subunit *NtR*, *mAChR-A*, *ChAT*) early in the glial trajectory. Cellular stress response
272 emerged later in the trajectory with up-regulation of heat shock proteins (*Hsp68*, *Hsp70Ab*),
273 while altered mitochondrial gene expression (*mt:ND5*, *mt:Col*) characterized astrocytes late in
274 the calculated trajectory. These findings suggest that altered astrocyte signaling (Fig. 6;
275 Supplemental Fig. S11) may emerge early in tauopathy pathogenesis and drive subsequent
276 cell-autonomous and non-cell autonomous stress responses and cytotoxicity. A complete list of
277 all differentially expressed glial genes, genes associated with Gene Ontology biological
278 processes, and trajectory-associated genes is provided in Supplemental Table S5.

279

280 **Gene regulatory networks in control and tau P251L knock-in Kenyon cells**

281 Kenyon cells are a major defined neuronal component of the central body of the *Drosophila*
282 brain (Fig. 4). Together with their output neurons (MBON), Kenyon cells play a central role in
283 learning and memory in the *Drosophila* brain (Heisenberg 2003; Modi et al. 2020); memory loss
284 is a key feature of human tauopathies (Grossman et al. 2023). Kenyon cells are cholinergic
285 (Barnstedt et al. 2016), a neuronal type that is selectively vulnerable in previously described fly
286 tauopathy models (Wittmann et al. 2001) and a pathway altered early in our trajectory analysis
287 (Fig. 7). Our cell-cell communication analyses suggested altered signaling in Kenyon cells, or
288 their output neurons, via multiple signaling pathways (Fig. 6; Supplemental Fig. 11). We
289 therefore focused next on gene expression in Kenyon cells. We identified three Kenyon cells
290 clusters, γ Kenyon cells, α/β Kenyon cells, and α'/β' Kenyon cells (Fig. 8A). Transposable

291 elements were up-regulated in all Kenyon cell clusters in tau P251L knock-in brains
292 (Supplemental Fig. S12A,C,E), as observed in other neuronal and glial clusters (Fig. 7,
293 Supplemental Fig. 7). Analysis of biological pathways associated with common up-regulated
294 and down-regulated genes in all three Kenyon cell clusters identified key biological processes
295 previously linked to tauopathy pathogenesis (Götz et al. 2019; Frost et al. 2015), including
296 control of DNA and RNA structure and metabolism (Fig. 8B), as well as many pathways without
297 prior links to tauopathy. A complete list of differentially expressed genes and associated
298 biological processes is given in Supplemental Table S6.

299 Given the multiple lines of evidence connecting tauopathy pathogenesis to Kenyon cell
300 function we next determined the gene regulatory networks controlling disease-associated
301 changes in gene expression in Kenyon cells. We implemented the SCENIC (Single-Cell
302 rEgulatory Network Inference and Clustering, Aibar et al. 2017) workflow on gene expression
303 data from control and tau P251L knock-in Kenyon cells. The top 10 regulons identified in
304 control compared to tauopathy model Kenyon cells are show in columns in the heat maps in Fig.
305 8C (control Kenyon cells) and Fig. 8D (tau P251L knock-in Kenyon cells). Regulons were largely
306 distinct in the two genotypes (Fig. 8C,D; Supplemental Table S7). The only shared transcription
307 factor among the top 10 regulons was *lola*. Even for the shared *lola* regulon, the gene
308 expression patterns per cell clustered and co-expressed with different transcription factors and
309 are different among Kenyon cells of control vs. tau P251L knock-in animals. The distinct gene
310 regulatory networks illustrated in the heatmap are concordant with altered gene expression (Fig.
311 8B) and cell-cell communication (Fig. 6) between control and tau P251L knock-in Kenyon cells.
312 The increase in *HSF*, *Stat92E* and *Parp* expression (Supplemental Fig. 13) and regulons (Fig.
313 8D) in brains of tauopathy model flies are consistent with elevated cellular stress, DNA damage
314 and cell death in aging neurons exposed to mutant tau P251L (Figs. 1,2).

315

316 **Discussion**

317 Here we present a new model of tauopathy in the experimentally facile model organism
318 *Drosophila* based on precise gene editing of the endogenous tau gene to introduce a mutation
319 orthologous to human proline 301 to leucine (P301L), the most common tau mutation in
320 frontotemporal dementia patients (Poorkaj et al. 2001). We observe age-dependent
321 neurodegeneration in our knock-in animals (Fig. 1C,D). Homozygous knock-in flies display early
322 and greater total levels of degeneration compared to heterozygous animals. These findings are
323 compatible with a toxic gain of function mechanism, as generally posited in familial
324 frontotemporal tauopathies (Goedert et al. 2012; Frost et al. 2015; Götz et al. 2019; Bardai et al.
325 2018b). However, given the important role of microtubules in neurodevelopment, a loss of
326 function component contribution cannot be excluded, even given the lack of clear
327 neurodegeneration in tau knockout mice (Harada et al. 1994; Dawson et al. 2001; Morris et al.
328 2013) and flies (Burnouf et al. 2016). As expected given that levels of mutant tau are controlled
329 by the endogenous tau promoter in our model compared with the strong exogenous promoter
330 systems employed in prior transgenic models, neurodegeneration in knock-in animals is
331 observed at older ages and is milder (Wittmann et al. 2001; Bardai et al. 2018b; Law et al.
332 2022). However, we do observe key biochemical and cellular pathologies previously described
333 in transgenic *Drosophila* tauopathy models, including metabolic dysfunction (Fig. 2A,B),
334 elevated levels of DNA damage (Fig. 2C-G), and abnormal cell cycle activation (Fig. 1E)
335 (Khurana et al. 2012; DuBoff et al. 2012; Bardai et al. 2018a; Khurana et al. 2006). Importantly,
336 these pathways are also perturbed in mouse tauopathy models and tauopathy patients
337 (Khurana et al. 2012; Götz et al. 2019; Frost et al. 2015; Andorfer et al. 2005; DuBoff et al.
338 2013; Welch and Tsai 2022; Herrup and Arendt 2002).

339 The similarities of our knock-in model to human tauopathies and prior overexpression
340 tauopathy models, recapitulated in a more faithful genetic knock-in context, motivated us to

341 perform a comprehensive transcriptional analysis in our tau P251L knock-in brains using single-
342 cell RNA sequencing. We recovered a large number (130,489) of high-quality cells, which
343 allowed us to identify the majority of previously annotated neuronal and glial groups from prior
344 single cell sequencing analyses in the adult fly brain (Li et al. 2022; Davie et al. 2018).
345 Comparing gene expression profiles between control and tau P251L knock-in animals revealed
346 pervasive dysregulation of genes in neuronal (Figs. 4,8) and glial (Fig. 7) subtypes and
347 throughout different anatomic regions (Fig. 4, and Supplemental Fig. 6). These findings are
348 consistent with prior single cell sequencing studies in flies overexpressing mutant human tau
349 (Praschberger et al. 2023; Wu et al. 2023). We observed regulation of both common and distinct
350 biological pathways when comparing differentially expressed genes across cell subtypes.
351 Transposable elements were notably up-regulated in the complete gene expression set, as well
352 as in specific anatomic regions and neuronal subtypes. These findings correlate with a
353 previously described functional role for transposable element mobilization in *Drosophila* models
354 of tauopathy, and in tauopathy patients (Sun et al. 2018; Guo et al. 2018). Mitochondrial
355 function has been strongly linked to neurotoxicity in tauopathies (Frost et al. 2015; Götz et al.
356 2019; DuBoff et al. 2013) and is a feature of our current model (Fig. 2). We accordingly
357 observed altered expression of mitochondrial genes and biological processes in the complete
358 expression data set (Fig. 4), as well as in separate analyses of the central body, optic lobe
359 (Supplemental Fig. 7), and Kenyon cells (Fig. 8, Supplementary Fig. S12). More importantly, we
360 observed significant alterations in multiple metabolic, cellular communication and biological
361 pathways not previously implicated in tauopathy pathogenesis (Figs. 4,5,6), which can now be
362 assessed in tauopathy models and patients for mechanistic relevance and ultimately therapeutic
363 targeting.

364 Cell type selectivity is a fundamental, and poorly understood, feature of human
365 neurodegenerative diseases, including tauopathies. Our protein interaction networks highlighted

366 regionally specific biology with predominantly distinct nodes appearing in the central body
367 compared to the optic lobe (Fig. 5). Comparative analysis of genes differentially expressed in
368 central body compared to the optic lobe are consistent with substantial regional differences in
369 the response to mutant tau expression with substantially greater numbers of unique compared
370 to common genes up-regulated in the central body vs. the optic lobe (Supplemental Fig. 7E).
371 Even within subgroups of Kenyon cells there are equivalent numbers or more uniquely up- or
372 down-regulated genes compared to commonly regulated genes (Fig. 8B). Our dataset thus
373 highlights a substantial set of genes that may contribute to selective neuronal susceptibility in
374 neurodegeneration, including many differentially regulated genes and processes not previously
375 linked to tau pathobiology.

376 Although tau is a predominantly neuronal protein (Götz et al. 2019; Goedert 2004;
377 Heidary and Fortini 2001), we observed significant alteration of glial gene expression in tau
378 P251L knock-in brains compared to controls (Figs. 4,7), suggestive of non-cell autonomous
379 control of glia cell function by neuronally expressed tau. Gene Ontology (Fig. 7A,B) and protein
380 interaction network (Fig. 5) analyses highlighted a number of metabolic processes altered in glia
381 by expression of toxic tau in neurons, including glutamate, lipid and amino acid metabolism
382 (Figs. 5,7). Glial uptake and detoxification of neurotransmitters and their metabolites, as well as
383 toxic lipid species, maintains neuronal function and viability. Lipid metabolism is further central
384 to energy production by glial cells, which support highly energy consuming neurons with active
385 synaptic transmission (Smolič et al. 2021; Jiwaji and Hardingham 2023). In addition to glial
386 processes previously implicating in controlling neuronal health, our transcriptional analysis
387 revealed new metabolic and signaling pathways in glia regulated by expression of mutant tau
388 (Fig. 7A-C), which can now be explored as non-cell autonomous mechanisms regulating
389 neuronal function and viability in tauopathy.

390 An effect of mutant tau expression enriched in neurons on glial gene expression implies
391 signaling, and possibly perturbed signaling, between the two cell types. Examination of
392 expression of 196 ligand-receptor pairs (Liu et al. 2022) indeed supported broad alterations in
393 glial-neuronal communication in tau P251L knock-in flies (Fig. 6, Supplemental Fig. S11), with
394 mutant tau expression perturbing synaptic plasticity, JAK-STAT, hippo, TNF- α , integrin and
395 EGFR signaling between perineurial cells, astrocytes and multiple neuronal subtypes. Although
396 prior studies have implicated glial signaling, for example the JAK-STAT pathway (Colodner and
397 Feany 2010), in non-cell autonomous control of neurotoxicity, the pervasive nature of the altered
398 signaling suggested by our single-cell transcriptional analyses is unexpected and provides
399 multiple targets for functional testing. Our findings further suggest that a systematic and broad
400 perturbation of intercellular signaling is present in tauopathy, which may require manipulation of
401 multiple pathways to correct and systems-level analysis to monitor.

402 Trajectory analysis has been widely used to order temporal events along developmental
403 pathways, but has less often been applied to neurodegenerative disease progression
404 (Karademir et al. 2022; Wang et al. 2022; Fitz et al. 2021; Dai et al. 2023). Given the evidence
405 for altered glial-neuronal communication in our tau knock-in model we assessed possible
406 trajectories in the four distinct subgroups of astrocytic glial cells that we defined. Using the
407 astrocyte cluster with the highest entropy as the root (Guo et al. 2017) we identified a single
408 astrocyte trajectory (Fig. 7G). Differential gene expression and Gene Ontology analyses across
409 the trajectory revealed altered expression of neurotransmitter and cell signaling genes first,
410 followed by altered cell stress responses, and finally mitochondrial changes (Fig. 7H,
411 Supplemental Table S5). A number of genes involved in cholinergic signaling were changed
412 early in the glial trajectory. We have previously demonstrated that cholinergic terminals are
413 preferentially vulnerable and degenerate early in a tauopathy model based on transgenic human
414 tau expression in flies (Wittmann et al. 2001). Our trajectory analysis may thus help identify

415 early events in glial-mediated neurodegeneration, including pathways not previously associated
416 with tauopathy (Supplemental Table S5). Glial pathways contributing to neurodegeneration are
417 increasingly recognized as attractive and understudied avenues for therapeutic intervention
418 (Jiwaji and Hardingham 2023). Identifying and intervening in early glial-neuronal signaling
419 events may prevent later, and possibly irreversible, neuronal damage.

420 Reversing pathological neuronal cell-autonomous programs may provide an alternative
421 or additional method of preventing neuronal dysfunction and death in tauopathies. We focused
422 on Kenyon cells as a group of neurons involved in the behaviorally relevant process of memory
423 and comprised of cholinergic neurons, a vulnerable cell type in *Drosophila* (Wittmann et al.
424 2001) and human (Ishida et al. 2015; Whitehouse et al. 1981) tauopathies to define
425 transcriptional programs driving neurodegeneration in response to mutant tau expression. As
426 expected by the multiple neuropathological and cell biological abnormalities present in our
427 knock-in model flies (Figs. 1,2), we observed substantially distinct regulons in tau P251L knock-
428 in Kenyon cells compared to controls (Fig. 8C,D). We identified regulons involved in stress
429 responses (*Hsf*, *Stat92E*), including the DNA damage response (*Parp*), as would be expected
430 from the presence of elevated DNA damage in Kenyon cells in our knock-in flies (Fig. 2E-G).
431 We recovered *nej*, the fly ortholog of vertebrate CREB-binding protein (also known as CBP) as
432 a top regulon induced in knock-in flies. Increasing levels of *nej*/CBP is beneficial in fly (Cutler et
433 al. 2015) and vertebrate (Caccamo et al. 2010) models relevant to Alzheimer's disease,
434 suggesting that up-regulation of *nej* may represent a protective response in Kenyon cells. We
435 also identified multiple regulons not previously associated with neurodegenerative tauopathies
436 (Fig. 8C,D). Therapeutic manipulation of these programs or key transcriptionally regulated
437 mediators will be attractive candidates for evaluation in patient tissue, patient derived cellular
438 models and vertebrate models of tauopathy.

439 The mechanisms transducing the effects of mutant tau on gene expression are likely
440 multiple and as yet only partially characterized. We have previously defined a cascade in which
441 cytosolic tau binds and stabilizes F-actin (Fulga et al. 2007), leading to signal transduction
442 through the LINC complex, nuclear lamin disruption (Frost et al. 2016) and consequent
443 chromatin relaxation (Frost et al. 2014) promoting aberrant transposable element activation and
444 neurodegeneration (Sun et al. 2018). Other cytosolic targets of tau may promote transcriptional
445 regulation through parallel mechanisms. For example, tau-mediated actin hyperstabilization
446 promotes mitochondrial dysfunction and excess production of oxidative free radicals by
447 interfering with mitochondrial dynamics (DuBoff et al. 2012). Oxidative stress may directly
448 contribute to elevated DNA damage in tauopathy (Bardai et al. 2018b; DuBoff et al. 2013; Götz
449 et al. 2019; Frost et al. 2016). However, although tau is best known as a cytosolic protein
450 involved in regulation of the cytoskeleton, a number of studies have demonstrated that tau can
451 also be detected in the nucleus (Loomis et al. 1990; Thurston et al. 1996; Cross et al. 2000),
452 where the protein binds DNA (Wei et al. 2008; Hua et al. 2003; Sjöberg et al. 2006; Bukar Maina
453 et al. 2016). Thus, tau may play a direct role in instructing the nuclear transcriptional programs
454 we have defined (Fig. 8C,D).

455 In summary, here we develop a genetically precise model of frontotemporal dementia
456 caused by the most common tau mutation found in patients and present a comprehensive
457 picture of gene expression changes and derived protein interaction, cell signaling and
458 transcriptional networks. We recapitulate neurodegeneration, metabolic dysfunction and DNA
459 damage, common features of human tauopathies (Goedert 2004; Götz et al. 2019; Welch and
460 Tsai 2022) and confirm that cellular pathways perturbed in overexpression tauopathy models
461 are also dysregulated in the more faithful genetic knock-in context. More importantly, our work
462 suggests previously unsuspected, pervasive alterations in glial-neuronal signaling in tauopathy

463 pathogenesis, implicates many new genes and pathways and provides a genetic model system
464 in which to test the new hypotheses our data suggests.

465

466 **Methods**

467 **Genetics and CRISPR-Cas9 editing**

468 The *Drosophila tau* gene is located on the 3rd chromosome. The guide RNAs targeting the *tau*
469 gene to mutate proline 251 to leucine were identified using Harvard Medical School's
470 DRSC/TRiP "find CRISPRs" tool. The gRNA '5 CCGGGAGGCGGGGACAAGAAGAT 3' was
471 cloned into pCDF3.1 plasmid and injected into the embryos of the TH_attP40 nos-Cas9 strain
472 along with a single-stranded oligo nucleotide donor. The single-stranded oligo nucleotide donor
473 was 150 bp in length and contained a C to T transition that resulted in alteration of the codon
474 CCG (proline) to CTG (leucine). Embryos were injected (BestGene Inc.) and founder flies
475 obtained. Founder flies were then balanced to obtain homozygous knock-in animals. The
476 mutation was confirmed by PCR. The genotype of knock-in animals in most experiments
477 (Figures 1,2C-E,4-8) was *elav-GAL4/+; tau-P251L knock-in* (homozygous or heterozygous for
478 *tau-P251L knock-in* as specified in figures and legends). In these experiments control animals
479 were *elav-GAL4/+*. In Fig. 2A,B the genotype of knock-in flies was $w^{1118}; tau-P251L knock-in /$
480 *tau-P251L knock-in* (homozygous) or $w^{1118}; tau-P251L knock-in / +$ (heterozygous) as specified
481 in the figure. In Fig. 2A,B the genotype of control flies was w^{1118} . The *elav-GAL4* line was
482 obtained from the Bloomington *Drosophila* Stock Center. Patrik Verstreken kindly provided tau
483 knockout flies. All crosses and aging were performed at 25°C.

484

485 **Assessment of neurodegeneration and metabolism**

486 For sectioning, adult flies were fixed in formalin at 1, 10 and 30 days of age and embedded in
487 paraffin. Vacuoles, PCNA and pH2Av levels were examined using previously described
488 methodology (Fulga et al. 2007; Frost et al. 2014) with additional details provided in the
489 Supplemental Methods. Primary antibodies used include pH2Av (Rockland, 600-401-914,
490 1:100), elav (DSHB, 9F8A9, 1:5), GAPDH (Thermo Fisher Scientific, MA5-15738, 1:1000) and
491 PCNA (DAKO, MO879, 1:500). A polyclonal antibody to *Drosophila* tau was prepared in rabbits
492 immunized with full length recombinant tau protein (Thermo Fisher Scientific) and was used at
493 1:5,000,000 for western blotting. For all histological analyses, at least 6 brains were analyzed
494 per genotype and time point. The comet assay and assessment of bioenergetics were
495 performed as previously described (Frost et al. 2014; Sarkar et al. 2020) with additional details
496 provided in the Supplemental Methods. The sample size (n), mean and SEM are given in the
497 figure legends. All statistical analyses were performed using GraphPad Prism 5.0. For
498 comparisons across more than 2 groups, one-way ANOVA with Tukey post-hoc analysis was
499 used. For comparison of 2 groups Student's *t*-tests were performed.

500

501 **Single-cell RNA sequencing (scRNA-seq) and downstream analyses**

502 A standard sample preparation (Li et al. 2017; Davie et al. 2018), raw data processing (Satija et
503 al. 2015) and downstream analyses such as cell cluster annotation (Hu et al. 2021) Gene
504 Ontology analysis (Kuleshov et al. 2016), protein-protein interaction network analysis (Tuncbag
505 et al. 2016), cell-cell communication analysis (Liu et al. 2022), trajectory analysis (Street et al.
506 2018) and gene regulatory network analysis (Van de Sande et al. 2020) were performed as
507 previously described. Detailed methods are presented in the Supplemental Methods.

508

509 **Data Access**

510 All raw and processed sequencing data generated in this study have been submitted to the
511 NCBI Gene Expression Omnibus (GEO; <https://www.ncbi.nlm.nih.gov/geo/>) under accession
512 number GSE223345. R code that was used to perform Seurat-based integration, trajectory, and
513 cell-cell interaction and PPI network analyses are available at GitHub ([https://github.com/bwh-
514 bioinformatics-hub/Single-cell-RNA-seq-of-the-CRISPR-engineered-endogenous-tauopathy-
515 model](https://github.com/bwh-bioinformatics-hub/Single-cell-RNA-seq-of-the-CRISPR-engineered-endogenous-tauopathy-model)) and in the Supplemental Code file.

516

517 **Competing Interest Statement**

518 The authors have no competing interests.

519

520 **Acknowledgments**

521 We thank Tingting Zhao for help with bioinformatics analyses and Yi Zhong for excellent
522 technical assistance. Fly stocks obtained from the Bloomington *Drosophila* Stock Center (NIH
523 P40OD018537) were used in this study. We thank Dr. Patrik Verstreken for providing the
524 *Drosophila* tau knockout line. Monoclonal antibodies were obtained from the Developmental
525 Studies Hybridoma Bank developed under the auspices of the NICHD and maintained by the
526 University of Iowa, Department of Biology, Iowa City, IA 52242. This research was funded by
527 NIH R01AG057331 and AG076214 and Aligning Science Across Parkinson's [Grant number
528 ASAP-000301] through the Michael J. Fox Foundation for Parkinson's Research (MJFF). For
529 the purpose of open access, the author has applied a CC BY public copyright license to all
530 Author Accepted Manuscripts arising from this submission.

531

532

533 **References**

- 534 Aibar S, González-Blas CB, Moerman T, Huynh-Thu VA, Imrichova H, Hulselmans G, Rambow
535 F, Marine J-C, Geurts P, Aerts J, et al. 2017. SCENIC: single-cell regulatory network
536 inference and clustering. *Nat Methods* **14**: 1083–1086.
- 537 Andorfer C, Acker CM, Kress Y, Hof PR, Duff K, Davies P. 2005. Cell-cycle reentry and cell
538 death in transgenic mice expressing nonmutant human tau isoforms. *J Neurosci* **25**:
539 5446–5454.
- 540 Bardai FH, Ordonez DG, Bailey RM, Hamm M, Lewis J, Feany MB. 2018a. Lrrk promotes tau
541 neurotoxicity through dysregulation of actin and mitochondrial dynamics. *PLoS Biol* **16**:
542 e2006265.
- 543 Bardai FH, Wang L, Mutreja Y, Yenjerla M, Gamblin TC, Feany MB. 2018b. A Conserved
544 Cytoskeletal Signaling Cascade Mediates Neurotoxicity of FTDP-17 Tau Mutations In
545 Vivo. *J Neurosci* **38**: 108–119.
- 546 Barnstedt O, Oswald D, Felsenberg J, Brain R, Moszynski J-P, Talbot CB, Perrat PN, Waddell S.
547 2016. Memory-Relevant Mushroom Body Output Synapses Are Cholinergic. *Neuron* **89**:
548 1237–1247.
- 549 Buchanan RL, Benzer S. 1993. Defective glia in the Drosophila brain degeneration mutant drop-
550 dead. *Neuron* **10**: 839–850.
- 551 Bukar Maina M, Al-Hilaly YK, Serpell LC. 2016. Nuclear Tau and Its Potential Role in
552 Alzheimer's Disease. *Biomolecules* **6**: 9.
- 553 Burnouf S, Grönke S, Augustin H, Dols J, Gorsky MK, Werner J, Kerr F, Alic N, Martinez P,
554 Partridge L. 2016. Deletion of endogenous Tau proteins is not detrimental in Drosophila.
555 *Sci Rep* **6**: 23102.
- 556 Butner KA, Kirschner MW. 1991. Tau protein binds to microtubules through a flexible array of
557 distributed weak sites. *J Cell Biol* **115**: 717–730.
- 558 Cabrales Fontela Y, Kadavath H, Biernat J, Riedel D, Mandelkow E, Zweckstetter M. 2017.
559 Multivalent cross-linking of actin filaments and microtubules through the microtubule-
560 associated protein Tau. *Nat Commun* **8**: 1981.
- 561 Caccamo A, Maldonado MA, Bokov AF, Majumder S, Oddo S. 2010. CBP gene transfer
562 increases BDNF levels and ameliorates learning and memory deficits in a mouse model
563 of Alzheimer's disease. *Proc Natl Acad Sci U S A* **107**: 22687–22692.
- 564 Chen EY, Tan CM, Kou Y, Duan Q, Wang Z, Meirelles GV, Clark NR, Ma'ayan A. 2013. Enrichr:
565 interactive and collaborative HTML5 gene list enrichment analysis tool. *BMC*
566 *Bioinformatics* **14**: 128.

- 567 Colodner KJ, Feany MB. 2010. Glial fibrillary tangles and JAK/STAT-mediated glial and
568 neuronal cell death in a *Drosophila* model of glial tauopathy. *J Neurosci* **30**: 16102–
569 16113.
- 570 Croset V, Treiber CD, Waddell S. 2018. Cellular diversity in the *Drosophila* midbrain revealed by
571 single-cell transcriptomics. *Elife* **7**: e34550.
- 572 Cross DC, Muñoz JP, Hernández P, Maccioni RB. 2000. Nuclear and cytoplasmic tau proteins
573 from human nonneuronal cells share common structural and functional features with
574 brain tau. *J Cell Biochem* **78**: 305–317.
- 575 Cutler T, Sarkar A, Moran M, Steffensmeier A, Puli OR, Mancini G, Tare M, Gogia N, Singh A.
576 2015. *Drosophila* Eye Model to Study Neuroprotective Role of CREB Binding Protein
577 (CBP) in Alzheimer's Disease. *PLoS One* **10**: e0137691.
- 578 Dai DL, Li M, Lee EB. 2023. Human Alzheimer's disease reactive astrocytes exhibit a loss of
579 homeostatic gene expression. *Acta Neuropathol Commun* **11**: 127.
- 580 Davie K, Janssens J, Koldere D, De Waegeneer M, Pech U, Kreft Ł, Aibar S, Makhzami S,
581 Christiaens V, Bravo González-Blas C, et al. 2018. A Single-Cell Transcriptome Atlas of
582 the Aging *Drosophila* Brain. *Cell* **174**: 982-998.e20.
- 583 Dawson HN, Ferreira A, Eyster MV, Ghoshal N, Binder LI, Vitek MP. 2001. Inhibition of neuronal
584 maturation in primary hippocampal neurons from tau deficient mice. *J Cell Sci* **114**:
585 1179–1187.
- 586 Dias-Santagata D, Fulga TA, Duttaroy A, Feany MB. 2007. Oxidative stress mediates tau-
587 induced neurodegeneration in *Drosophila*. *J Clin Invest* **117**: 236–245.
- 588 DuBoff B, Feany M, Götz J. 2013. Why size matters - balancing mitochondrial dynamics in
589 Alzheimer's disease. *Trends Neurosci* **36**: 325–335.
- 590 DuBoff B, Götz J, Feany MB. 2012. Tau promotes neurodegeneration via DRP1 mislocalization
591 in vivo. *Neuron* **75**: 618–632.
- 592 Dumont M, Stack C, Elipenahli C, Jainuddin S, Gerges M, Starkova NN, Yang L, Starkov AA,
593 Beal F. 2011. Behavioral deficit, oxidative stress, and mitochondrial dysfunction precede
594 tau pathology in P301S transgenic mice. *FASEB J* **25**: 4063–4072.
- 595 Feany MB, Dickson DW. 1996. Neurodegenerative disorders with extensive tau pathology: a
596 comparative study and review. *Ann Neurol* **40**: 139–148.
- 597 Feany MB, Quinn WG. 1995. A neuropeptide gene defined by the *Drosophila* memory mutant
598 amnesiac. *Science* **268**: 869–873.

- 599 Fitz NF, Nam KN, Wolfe CM, Letronne F, Playso BE, Iordanova BE, Kozai TDY, Biedrzycki RJ,
600 Kagan VE, Tyurina YY, et al. 2021. Phospholipids of APOE lipoproteins activate
601 microglia in an isoform-specific manner in preclinical models of Alzheimer's disease. *Nat*
602 *Commun* **12**: 3416.
- 603 Frost B, Bardai FH, Feany MB. 2016. Lamin Dysfunction Mediates Neurodegeneration in
604 Tauopathies. *Curr Biol* **26**: 129–136.
- 605 Frost B, Götz J, Feany MB. 2015. Connecting the dots between tau dysfunction and
606 neurodegeneration. *Trends Cell Biol* **25**: 46–53.
- 607 Frost B, Hemberg M, Lewis J, Feany MB. 2014. Tau promotes neurodegeneration through
608 global chromatin relaxation. *Nat Neurosci* **17**: 357–366.
- 609 Fulga TA, Elson-Schwab I, Khurana V, Steinhilb ML, Spires TL, Hyman BT, Feany MB. 2007.
610 Abnormal bundling and accumulation of F-actin mediates tau-induced neuronal
611 degeneration in vivo. *Nat Cell Biol* **9**: 139–148.
- 612 Ghetti B, Oblak AL, Boeve BF, Johnson KA, Dickerson BC, Goedert M. 2015. Invited review:
613 Frontotemporal dementia caused by *microtubule-associated protein tau* gene (*MAPT*)
614 mutations: a chameleon for neuropathology and neuroimaging: *MAPT* mutations and
615 FTD. *Neuropathology and Applied Neurobiology* **41**: 24–46.
- 616 Goedert M. 2004. Tau protein and neurodegeneration. *Semin Cell Dev Biol* **15**: 45–49.
- 617 Goedert M, Ghetti B, Spillantini MG. 2012. Frontotemporal dementia: implications for
618 understanding Alzheimer disease. *Cold Spring Harb Perspect Med* **2**: a006254.
- 619 Goedert M, Jakes R. 2005. Mutations causing neurodegenerative tauopathies. *Biochim Biophys*
620 *Acta* **1739**: 240–250.
- 621 Goodman LD, Bellen HJ. 2022. Recent insights into the role of glia and oxidative stress in
622 Alzheimer's disease gained from *Drosophila*. *Curr Opin Neurobiol* **72**: 32–38.
- 623 Götz J, Chen F, Barmettler R, Nitsch RM. 2001. Tau filament formation in transgenic mice
624 expressing P301L tau. *J Biol Chem* **276**: 529–534.
- 625 Götz J, Halliday G, Nisbet RM. 2019. Molecular Pathogenesis of the Tauopathies. *Annu Rev*
626 *Pathol* **14**: 239–261.
- 627 Grossman M, Seeley WW, Boxer AL, Hillis AE, Knopman DS, Ljubenov PA, Miller B, Piguet O,
628 Rademakers R, Whitwell JL, et al. 2023. Frontotemporal lobar degeneration. *Nat Rev*
629 *Dis Primers* **9**: 40.
- 630 Guo C, Jeong H-H, Hsieh Y-C, Klein H-U, Bennett DA, De Jager PL, Liu Z, Shulman JM. 2018.
631 Tau Activates Transposable Elements in Alzheimer's Disease. *Cell Rep* **23**: 2874–2880.

- 632 Guo M, Bao EL, Wagner M, Whitsett JA, Xu Y. 2017. SLICE: determining cell differentiation and
633 lineage based on single cell entropy. *Nucleic Acids Res* **45**: e54.
- 634 Guven-Ozkan T, Davis RL. 2014. Functional neuroanatomy of *Drosophila* olfactory memory
635 formation. *Learn Mem* **21**: 519–526.
- 636 Harada A, Oguchi K, Okabe S, Kuno J, Terada S, Ohshima T, Sato-Yoshitake R, Takei Y, Noda
637 T, Hirokawa N. 1994. Altered microtubule organization in small-calibre axons of mice
638 lacking tau protein. *Nature* **369**: 488–491.
- 639 Heidary G, Fortini ME. 2001. Identification and characterization of the *Drosophila* tau homolog.
640 *Mech Dev* **108**: 171–178.
- 641 Heisenberg M. 2003. Mushroom body memoir: from maps to models. *Nat Rev Neurosci* **4**: 266–
642 275.
- 643 Heisenberg M, Böhl K. 1979. Isolation of Anatomical Brain Mutants of *Drosophila* by Histological
644 Means. *Zeitschrift für Naturforschung C* **34**: 143–147.
- 645 Herrup K, Arendt T. 2002. Re-expression of cell cycle proteins induces neuronal cell death
646 during Alzheimer's disease. *J Alzheimers Dis* **4**: 243–247.
- 647 Hong S-T, Choi K-W. 2013. TCTP directly regulates ATM activity to control genome stability and
648 organ development in *Drosophila melanogaster*. *Nat Commun* **4**: 2986.
- 649 Hua Q, He RQ, Haque N, Qu MH, del Carmen Alonso A, Grundke-Iqbal I, Iqbal K. 2003.
650 Microtubule associated protein tau binds to double-stranded but not single-stranded
651 DNA. *Cell Mol Life Sci* **60**: 413–421.
- 652 Husseman JW, Nochlin D, Vincent I. 2000. Mitotic activation: a convergent mechanism for a
653 cohort of neurodegenerative diseases. *Neurobiol Aging* **21**: 815–828.
- 654 Ishida C, Kobayashi K, Kitamura T, Ujike H, Iwasa K, Yamada M. 2015. Frontotemporal
655 dementia with parkinsonism linked to chromosome 17 with the MAPT R406W mutation
656 presenting with a broad distribution of abundant senile plaques. *Neuropathology* **35**: 75–
657 82.
- 658 Jiwaji Z, Hardingham GE. 2023. The consequences of neurodegenerative disease on neuron-
659 astrocyte metabolic and redox interactions. *Neurobiol Dis* **185**: 106255.
- 660 Karademir D, Todorova V, Ebner LJA, Samardzija M, Grimm C. 2022. Single-cell RNA
661 sequencing of the retina in a model of retinitis pigmentosa reveals early responses to
662 degeneration in rods and cones. *BMC Biol* **20**: 86.

- 663 Khurana V, Lu Y, Steinhilb ML, Oldham S, Shulman JM, Feany MB. 2006. TOR-mediated cell-
664 cycle activation causes neurodegeneration in a *Drosophila* tauopathy model. *Curr Biol*
665 **16**: 230–241.
- 666 Khurana V, Merlo P, DuBoff B, Fulga TA, Sharp KA, Campbell SD, Götz J, Feany MB. 2012. A
667 neuroprotective role for the DNA damage checkpoint in tauopathy. *Aging Cell* **11**: 360–
668 362.
- 669 Lapytsko A, Kollarovic G, Ivanova L, Studencka M, Schaber J. 2015. FoCo: a simple and robust
670 quantification algorithm of nuclear foci. *BMC Bioinformatics* **16**: 392.
- 671 Law AD, Cassar M, Long DM, Chow ES, Giebultowicz JM, Venkataramanan A, Strauss R,
672 Kretzschmar D. 2022. FTD-associated mutations in Tau result in a combination of
673 dominant and recessive phenotypes. *Neurobiol Dis* **170**: 105770.
- 674 Lee G, Neve RL, Kosik KS. 1989. The microtubule binding domain of tau protein. *Neuron* **2**:
675 1615–1624.
- 676 Lee JA, Hall B, Allsop J, Alqarni R, Allen SP. 2021. Lipid metabolism in astrocytic structure and
677 function. *Semin Cell Dev Biol* **112**: 123–136.
- 678 Lewis J, Dickson DW, Lin WL, Chisholm L, Corral A, Jones G, Yen SH, Sahara N, Skipper L,
679 Yager D, et al. 2001. Enhanced neurofibrillary degeneration in transgenic mice
680 expressing mutant tau and APP. *Science* **293**: 1487–1491.
- 681 Li H, Janssens J, De Waegeneer M, Kolluru SS, Davie K, Gardeux V, Saelens W, David FPA,
682 Brbić M, Spanier K, et al. 2022. Fly Cell Atlas: A single-nucleus transcriptomic atlas of
683 the adult fruit fly. *Science* **375**: eabk2432.
- 684 Liu Y, Li JSS, Rodiger J, Comjean A, Attrill H, Antonazzo G, Brown NH, Hu Y, Perrimon N.
685 2022. FlyPhoneDB: an integrated web-based resource for cell-cell communication
686 prediction in *Drosophila*. *Genetics* **220**: iyab235.
- 687 Loomis PA, Howard TH, Castleberry RP, Binder LI. 1990. Identification of nuclear tau isoforms
688 in human neuroblastoma cells. *Proc Natl Acad Sci U S A* **87**: 8422–8426.
- 689 Madigan JP, Chotkowski HL, Glaser RL. 2002. DNA double-strand break-induced
690 phosphorylation of *Drosophila* histone variant H2Av helps prevent radiation-induced
691 apoptosis. *Nucleic Acids Res* **30**: 3698–3705.
- 692 Modi MN, Shuai Y, Turner GC. 2020. The *Drosophila* Mushroom Body: From Architecture to
693 Algorithm in a Learning Circuit. *Annu Rev Neurosci* **43**: 465–484.
- 694 Morris M, Hamto P, Adame A, Devidze N, Masliah E, Mucke L. 2013. Age-appropriate cognition
695 and subtle dopamine-independent motor deficits in aged tau knockout mice. *Neurobiol*
696 *Aging* **34**: 1523–1529.

- 697 Nedergaard M, Verkhratsky A. 2012. Artifact versus reality--how astrocytes contribute to
698 synaptic events. *Glia* **60**: 1013–1023.
- 699 Neville KE, Bosse TL, Klekos M, Mills JF, Weicksel SE, Waters JS, Tipping M. 2018. A novel ex
700 vivo method for measuring whole brain metabolism in model systems. *J Neurosci*
701 *Methods* **296**: 32–43.
- 702 Ordonez DG, Lee MK, Feany MB. 2018. α -synuclein Induces Mitochondrial Dysfunction through
703 Spectrin and the Actin Cytoskeleton. *Neuron* **97**: 108-124.e6.
- 704 Poorkaj P, Grossman M, Steinbart E, Payami H, Sadovnick A, Nochlin D, Tabira T, Trojanowski
705 JQ, Borson S, Galasko D, et al. 2001. Frequency of tau gene mutations in familial and
706 sporadic cases of non-Alzheimer dementia. *Arch Neurol* **58**: 383–387.
- 707 Praschberger R, Kuenen S, Schoovaerts N, Kaempf N, Singh J, Janssens J, Swerts J,
708 Nachman E, Calatayud C, Aerts S, et al. 2023. Neuronal identity defines α -synuclein and
709 tau toxicity. *Neuron* **111**: 1577-1590.e11.
- 710 Rhein V, Song X, Wiesner A, Ittner LM, Baysang G, Meier F, Ozmen L, Bluethmann H, Dröse S,
711 Brandt U, et al. 2009. Amyloid-beta and tau synergistically impair the oxidative
712 phosphorylation system in triple transgenic Alzheimer's disease mice. *Proc Natl Acad*
713 *Sci U S A* **106**: 20057–20062.
- 714 Sarkar S, Murphy MA, Dammer EB, Olsen AL, Rangaraju S, Fraenkel E, Feany MB. 2020.
715 Comparative proteomic analysis highlights metabolic dysfunction in α -synucleinopathy.
716 *NPJ Parkinsons Dis* **6**: 40.
- 717 Schulz L, Ramirez P, Lemieux A, Gonzalez E, Thomson T, Frost B. 2023. Tau-Induced
718 Elevation of the Activity-Regulated Cytoskeleton Associated Protein Arc1 Causally
719 Mediates Neurodegeneration in the Adult Drosophila Brain. *Neuroscience* **518**: 101–111.
- 720 Shanbhag NM, Evans MD, Mao W, Nana AL, Seeley WW, Adame A, Rissman RA, Masliah E,
721 Mucke L. 2019. Early neuronal accumulation of DNA double strand breaks in
722 Alzheimer's disease. *Acta Neuropathol Commun* **7**: 77.
- 723 Sjöberg MK, Shestakova E, Mansuroglu Z, Maccioni RB, Bonnefoy E. 2006. Tau protein binds
724 to pericentromeric DNA: a putative role for nuclear tau in nucleolar organization. *J Cell*
725 *Sci* **119**: 2025–2034.
- 726 Smolič T, Zorec R, Vardjan N. 2021. Pathophysiology of Lipid Droplets in Neuroglia.
727 *Antioxidants (Basel)* **11**: 22.
- 728 Street K, Risso D, Fletcher RB, Das D, Ngai J, Yosef N, Purdom E, Dudoit S. 2018. Slingshot:
729 cell lineage and pseudotime inference for single-cell transcriptomics. *BMC Genomics* **19**:
730 477.

- 731 Sun W, Samimi H, Gamez M, Zare H, Frost B. 2018. Pathogenic tau-induced piRNA depletion
732 promotes neuronal death through transposable element dysregulation in
733 neurodegenerative tauopathies. *Nat Neurosci* **21**: 1038–1048.
- 734 Thadathil N, Delotterie DF, Xiao J, Hori R, McDonald MP, Khan MM. 2021. DNA Double-Strand
735 Break Accumulation in Alzheimer's Disease: Evidence from Experimental Models and
736 Postmortem Human Brains. *Mol Neurobiol* **58**: 118–131.
- 737 Thurston VC, Zinkowski RP, Binder LI. 1996. Tau as a nucleolar protein in human nonneural
738 cells in vitro and in vivo. *Chromosoma* **105**: 20–30.
- 739 Tuncbag N, Braunstein A, Pagnani A, Huang S-SC, Chayes J, Borgs C, Zecchina R, Fraenkel
740 E. 2013. Simultaneous reconstruction of multiple signaling pathways via the prize-
741 collecting steiner forest problem. *J Comput Biol* **20**: 124–136.
- 742 Verkhatsky A, Sofroniew MV, Messing A, deLanerolle NC, Rempe D, Rodríguez JJ,
743 Nedergaard M. 2012. Neurological diseases as primary gliopathies: a reassessment of
744 neurocentrism. *ASN Neuro* **4**.
- 745 von Bergen M, Friedhoff P, Biernat J, Heberle J, Mandelkow EM, Mandelkow E. 2000.
746 Assembly of tau protein into Alzheimer paired helical filaments depends on a local
747 sequence motif ((306)VQIVYK(311)) forming beta structure. *Proc Natl Acad Sci U S A*
748 **97**: 5129–5134.
- 749 Wang S, Sudan R, Peng V, Zhou Y, Du S, Yuede CM, Lei T, Hou J, Cai Z, Cella M, et al. 2022.
750 TREM2 drives microglia response to amyloid- β via SYK-dependent and -independent
751 pathways. *Cell* **185**: 4153-4169.e19.
- 752 Wei Y, Qu M-H, Wang X-S, Chen L, Wang D-L, Liu Y, Hua Q, He R-Q. 2008. Binding to the
753 minor groove of the double-strand, tau protein prevents DNA from damage by
754 peroxidation. *PLoS One* **3**: e2600.
- 755 Welch G, Tsai L-H. 2022. Mechanisms of DNA damage-mediated neurotoxicity in
756 neurodegenerative disease. *EMBO Rep* **23**: e54217.
- 757 Whitehouse PJ, Price DL, Clark AW, Coyle JT, DeLong MR. 1981. Alzheimer disease: evidence
758 for selective loss of cholinergic neurons in the nucleus basalis. *Ann Neurol* **10**: 122–126.
- 759 Wittmann CW, Wszolek MF, Shulman JM, Salvaterra PM, Lewis J, Hutton M, Feany MB. 2001.
760 Tauopathy in *Drosophila*: neurodegeneration without neurofibrillary tangles. *Science*
761 **293**: 711–714.
- 762 Wu T, Deger JM, Ye H, Guo C, Dhindsa J, Pekarek BT, Al-Ouran R, Liu Z, Al-Ramahi I, Botas
763 J, et al. 2023. Tau polarizes an aging transcriptional signature to excitatory neurons and
764 glia. *Elife* **12**: e85251.

765 Yoshiyama Y, Higuchi M, Zhang B, Huang S-M, Iwata N, Saido TC, Maeda J, Suhara T,
766 Trojanowski JQ, Lee VM-Y. 2007. Synapse loss and microglial activation precede
767 tangles in a P301S tauopathy mouse model. *Neuron* **53**: 337–351.

768

769

770 **Figure legends**

771 **Figure 1. CRISPR-Cas9-mediated knock-in model of frontotemporal dementia in**
772 ***Drosophila*.** CRISPR-Cas9 gene editing strategy to knock in the human tau P301L homologous
773 mutation in *Drosophila*, tau P251L, located in exon 5 of *Drosophila* tau (*A*). Successful mutation
774 in homozygous tau P251L knock-in flies (*B*). Hematoxylin and eosin staining reveals evidence of
775 neurodegeneration as seen by increased number of brain vacuoles (arrowheads) with age in
776 homozygous and heterozygous knock-in animals (*C,D*). Scale bar represents 10 μm (*C*).
777 Neurodegeneration is accompanied by abnormal cell cycle reentry as marked by proliferating
778 cell nuclear antigen (PCNA) staining (*E*). Flies are 30 days old in (*C*) and the age indicated in
779 the figure labels in (*D,E*). $n = 6$ per genotype and time point (*D,E*). Data are presented as mean
780 \pm SD. *** = $P < 0.001$, one-way ANOVA with Tukey post-hoc analysis.

781 **Figure 2. Mitochondrial dysfunction and DNA damage in tau P251L knock-in brains.**
782 Decreased oxygen consumption rate (OCR) (*A*) and shift to a quiescent metabolic phenotype as
783 indicated by plotting the OCR vs. the extracellular acidification rate (ECAR) (*B*) in homozygous
784 and heterozygous tau P251L knock-in brains compared to controls. $n = 6$ per genotype.
785 Elevated levels of DNA damage in tau P251L knock-in brains as indicated by increased tail
786 length (*C*, arrowheads, *D*) following electrophoresis of nuclei from dissociated brains in the
787 comet assay. $n = 3$ per genotype. Increase in the number of Kenyon cells neurons (*E*, identified
788 by the neuronal marker elav) containing DNA double-strand breaks as marked by pH2Av foci
789 (*E*, arrowheads; arrows indicate neuronal nuclei with more than two foci) in histological sections
790 of mushroom bodies (Kenyon cells) from tau P251L knock-in animals, as quantified in (*F,G*). $n =$
791 6 per genotype and time point. Scale bars represent 5 μm . Flies are 10 days old in (*A-D*), 30
792 days old in (*E*) and the age indicated in the figure labels in (*F,G*). Data are presented as mean \pm
793 SD. *** = $P < 0.001$, one-way ANOVA with Tukey post-hoc analysis.

794

795 **Figure 3. Single-cell RNA sequencing of tau P251L knock-in brains.** Schematic of the
796 single-cell RNA sequencing analysis pipeline (A). Following dissection, brains were dissociated
797 in the enzymatic solutions and the single-cell suspension was encapsulated by 10x chromium
798 platform. The 10x libraries were prepared, sequenced and after quality control, data was
799 analyzed. UMAP representation of the 6 integrated sc-RNA sequencing runs, 3 control and 3
800 tau P251L knock-in (B). The integrated dataset contains 130,489 cells, and 26 clusters out of 29
801 were annotated. Percentage expression heatmap of the highly expressed marker genes within
802 all clusters (C). Flies are 10 days old.

803

804 **Figure 4. Differential gene expression and enrichment analysis of the scRNA-seq dataset**
805 **in tau P251L knock-in brains compared to controls.** The number of differentially expressed
806 genes (DEGs), both up-regulated and down-regulated genes, in all the annotated clusters of tau
807 P251L knock-in brains compared to controls (A). Results are displayed across three major
808 anatomic and functional classes of cells: 1) central body containing three clusters of Kenyon
809 cells (KC), mushroom body output neurons and pox neurons, 2) optic lobe neurons containing
810 lamina, medullary and lobula neurons clusters, and 3) glia cells containing astrocytes and
811 perineurial clusters. Heatmap of the top 50 up-regulated (B) and down-regulated (C) genes in all
812 the clusters of tau P251L knock-in brains compared to controls (Supplemental Table S3). Gene
813 Ontology (GO) enrichment analysis identified top up-regulated and down-regulated biological
814 processes (BP), molecular functions (MF), and cellular components (CC) (D). Analysis of
815 human disease associated genes revealed top up-regulated and down-regulated disease-
816 associated gene sets (E). Score represents the combined score $c = \log(p) * z$ (Chen et al. 2013).

817

818 **Figure 5. Protein interaction networks enriched in the central body, optic lobe and glia in**
819 **tau P251L knock-in brains compared to controls.** Protein interaction networks are largely
820 distinct among central body neurons, optic lobe neurons and glia. Subnetworks including nodes
821 enriched for protein catabolism (central body), electron transport chain (optic lobe) or fatty acid
822 metabolism (glia) are highlighted. Interaction strength displayed in gray shows the stringency of
823 the interaction: the lower the strength, the stronger the interaction.

824

825 **Figure 6: Cell-cell communication analysis predicts altered signaling in tau P251L knock-**
826 **in brains compared to controls.** Altered ligand and receptor expression predicts regulation of
827 synaptic plasticity signaling mainly via perineurial glial cells in control brains (A). Signaling from
828 perineurial glia is significantly reduced in tau P251L knock-in brains as predicted by levels of
829 spaetzle ligand and kekkon receptor (B). JAK-STAT signaling, as predicted by expression of the
830 upd2 ligand and dome receptor, mediated by perineurial glia in control brains (C), is
831 substantially reduced in brains from tau P251L knock-in animals (D). Hippo signaling, indicated
832 by expression of ds ligand and fat receptor, is up-regulated in astrocytes of flies expressing
833 P251L mutant tau compared to controls (E,F). Predicted TNF- α signaling from ligand eiger to
834 receptor wengen is increased in astrocytes of tau P251L knock-in flies (G,H). In panels
835 (B,D,F,H) the interactions from and to the specified cell types are indicated on the x-axis, while
836 the size of the circle indicates the P value and the intensity of the blue color illustrates the
837 interaction score as defined in the figure label below the panels.

838

839 **Figure 7: Gene expression and trajectory analysis in glia.** Differentially regulated genes,
840 both upregulated and down-regulated, in perineurial glia of tau P251L knock-in brains compared
841 to controls (A). Gene Ontology analysis shows biological processes associated with the up-

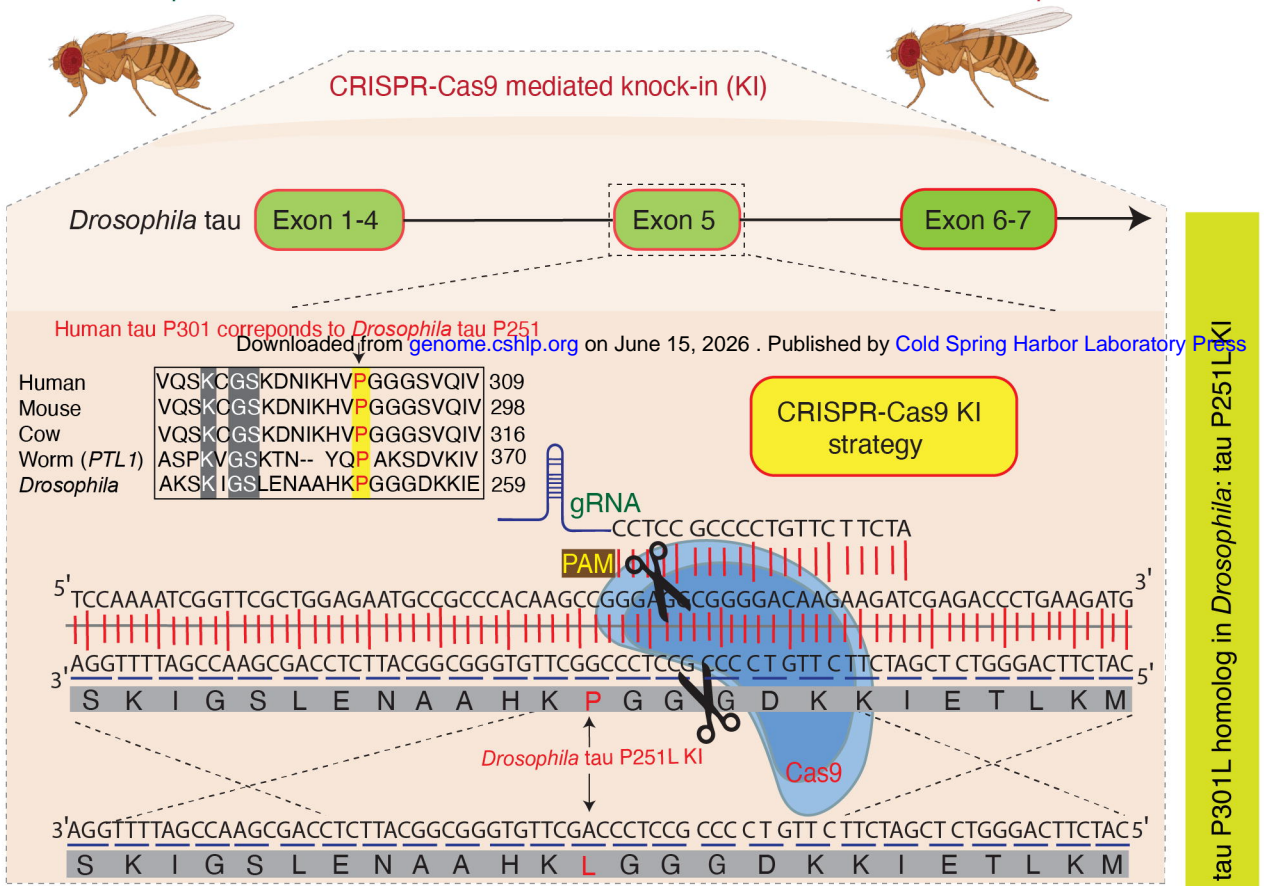
842 regulated and down-regulated genes in perineurial glia from tau P251L knock-in brains
843 compared to controls (*B*). Differentially regulated genes, both upregulated and down-regulated, in
844 astrocytes of tau P251L knock-in brains compared to controls (*C*). Gene Ontology analysis
845 shows biological process associated with upregulated and down-regulated genes in astrocytes of
846 tau P251L knock-in brains (*D*). All dots on the volcano plots are significant at $FDR < 0.05$ and
847 $\log_2FC > 0.25$ for up-regulated and < -0.25 for down-regulated genes. Score represents the
848 combined score $c = \log(p)*z$ (Chen et al. 2013). Astrocytes from both control and tau P251L
849 knock-in brains were further subclustered into 4 groups. Entropy analysis to define the root for
850 trajectory analysis revealed cluster 1 to have the highest entropy (*E,F*). Slingshot trajectory
851 analysis on astrocyte clusters identified a single lineage passing sequentially from clusters 1 to
852 2, 3, and 0 (*G*). Differential gene expression between astrocyte subclusters adjacent in
853 pseudotime were used to cluster genes along the pseudotime trajectory (*H*). Each row in the
854 heat map represents a gene. The columns are astrocyte subclusters arranged according
855 according to pseudotime from left to right. Examples of differentially regulated genes from
856 enriched Gene Ontology biological processes are shown on the calculated trajectory (*H*).

857

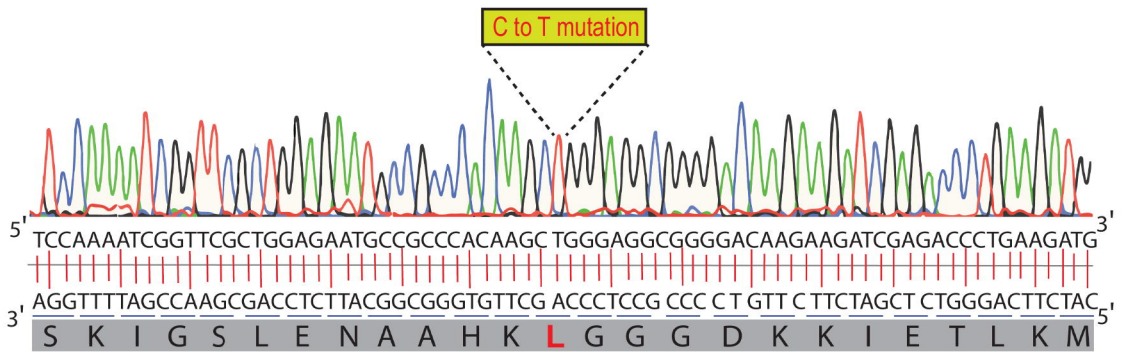
858 **Figure 8: Gene expression and regulatory networks in Kenyon cells.** Three Kenyon cell
859 (KC) clusters, γ -KC, $\alpha\beta$ -KC, and $\alpha'\beta'$ -KC, and biological process based on the common
860 upregulated and down-regulated genes in Kenyon cell clusters in tau P251L knock-in brains
861 (*A,B*). Score represents the combined score $c = \log(p)*z$ (Chen et al. 2013). Control and tau
862 P251L knock-in Kenyon cells were clustered separately using SCENIC gene regulatory network
863 analysis to identify regulons. The top 10 regulons identified by SCENIC gene regulatory network
864 analysis in control (*C*) and tau P251L knock-in (*C*) Kenyon cells (*C*) are presented in the
865 heatmaps. Each row represents a Kenyon cell; each column is a regulon.

wt tau *Drosophila*

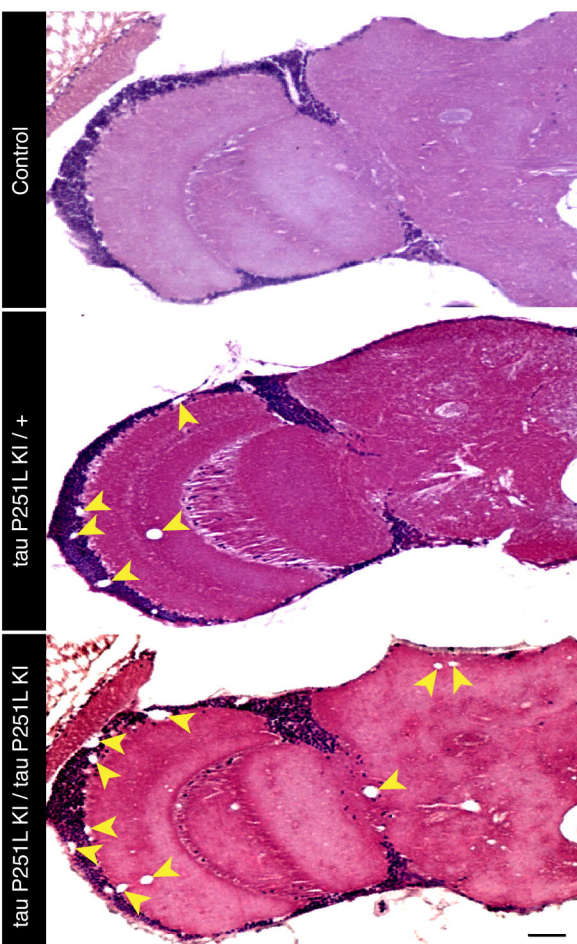
tau P251L KI *Drosophila*



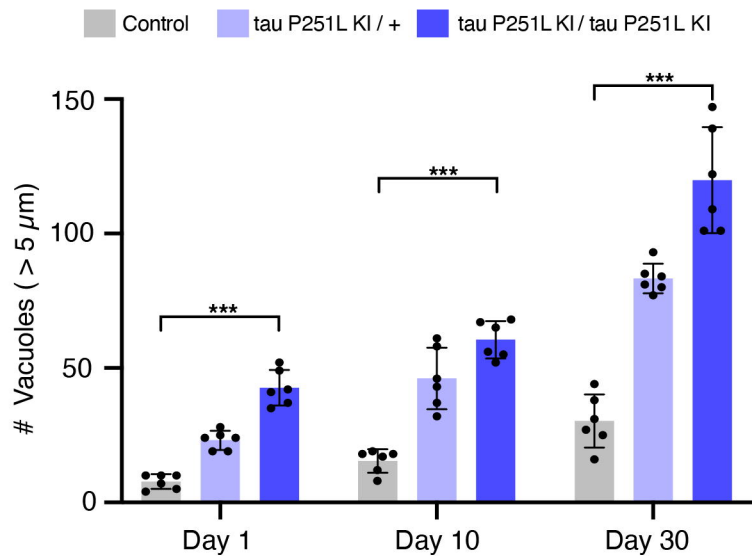
B



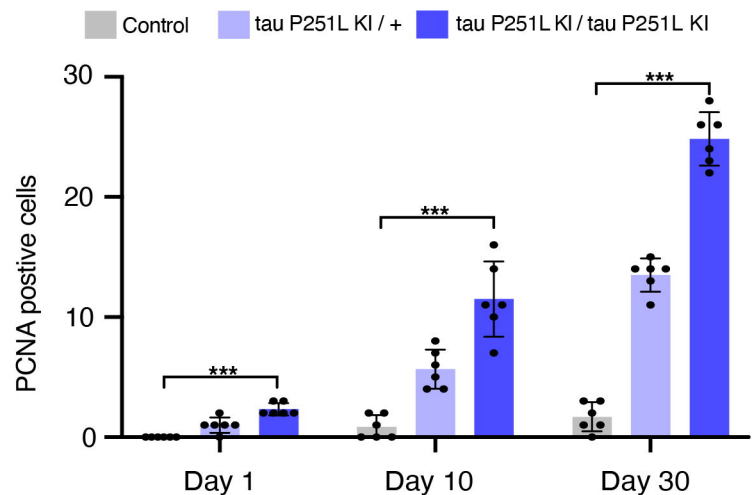
C

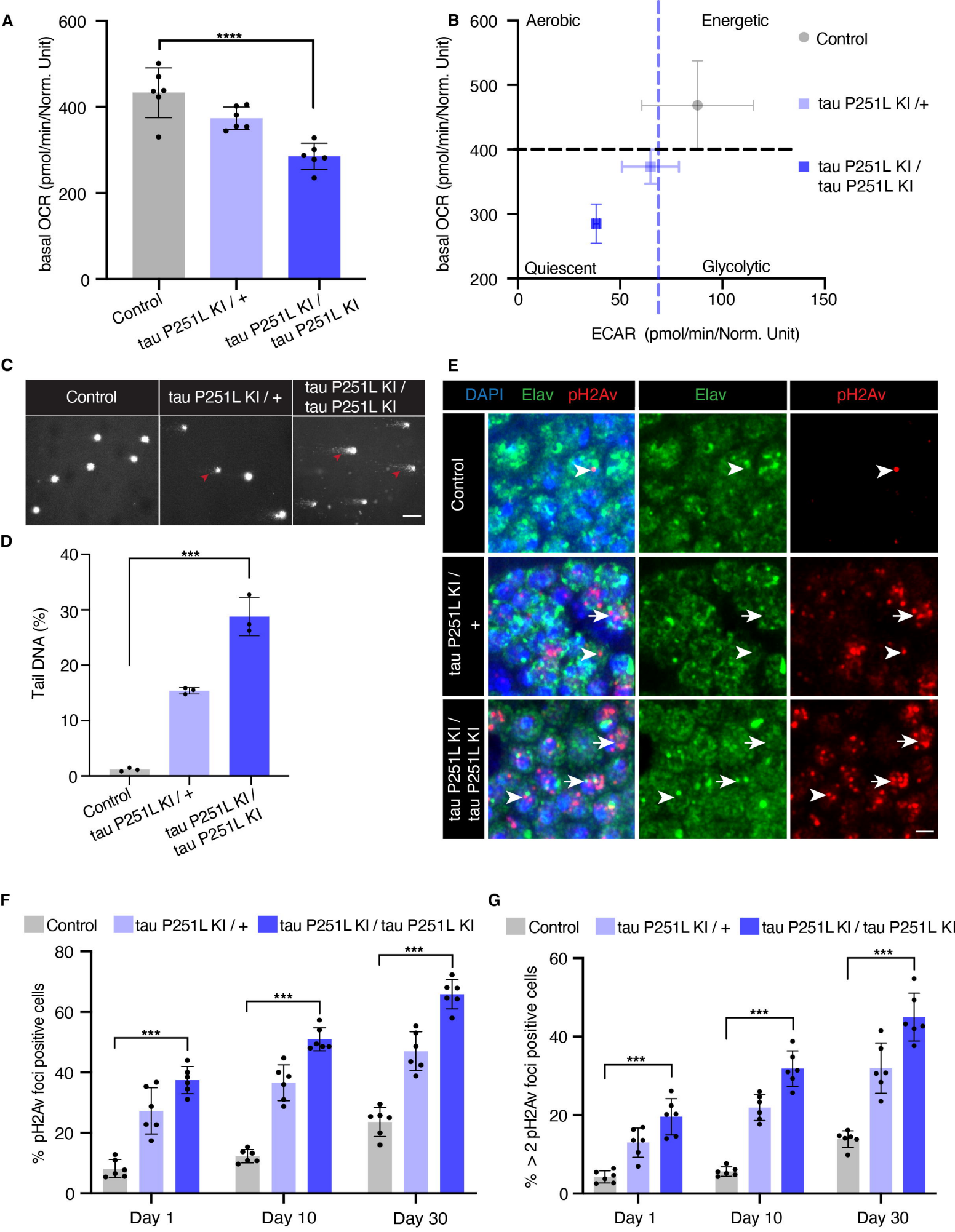


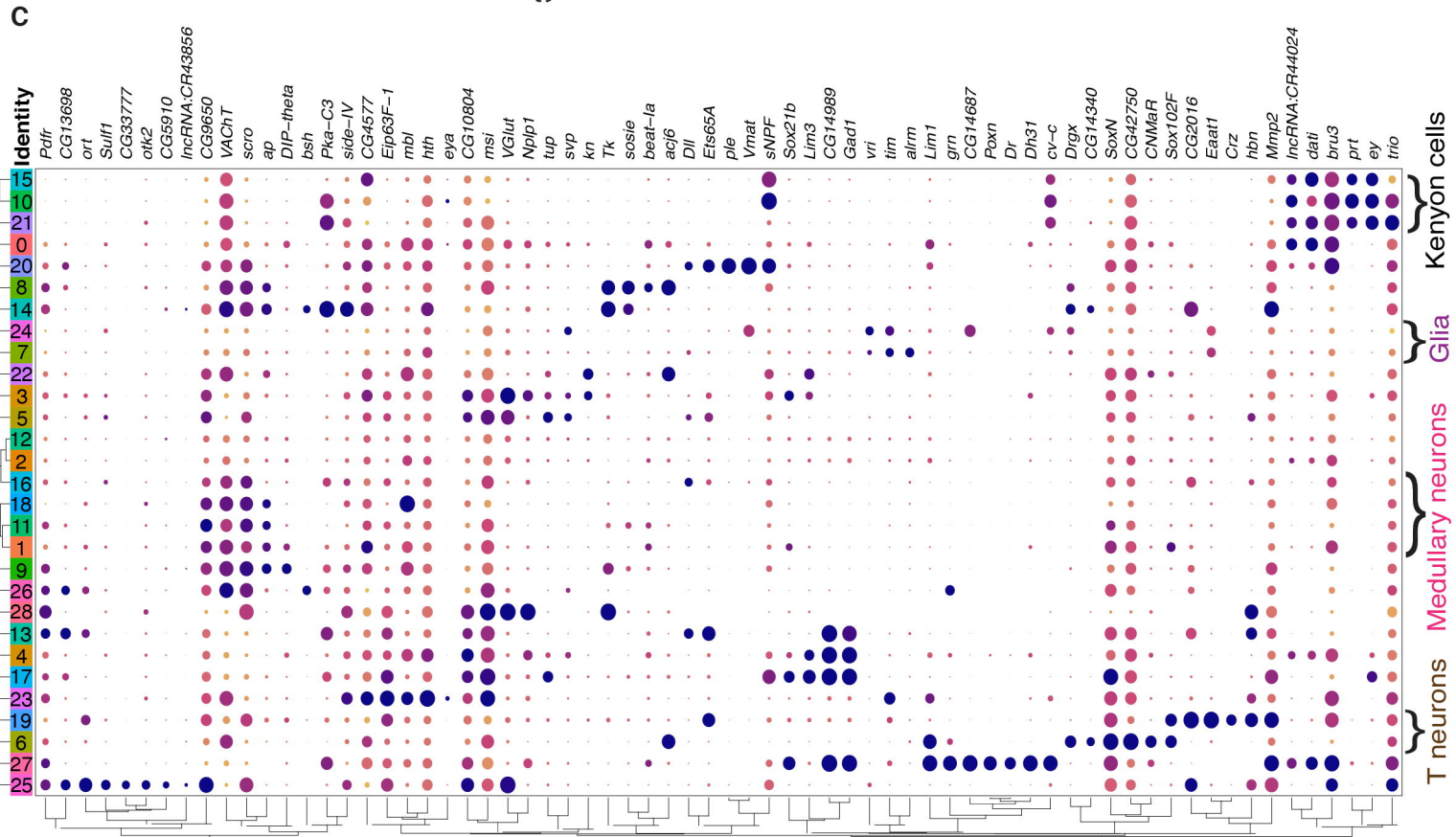
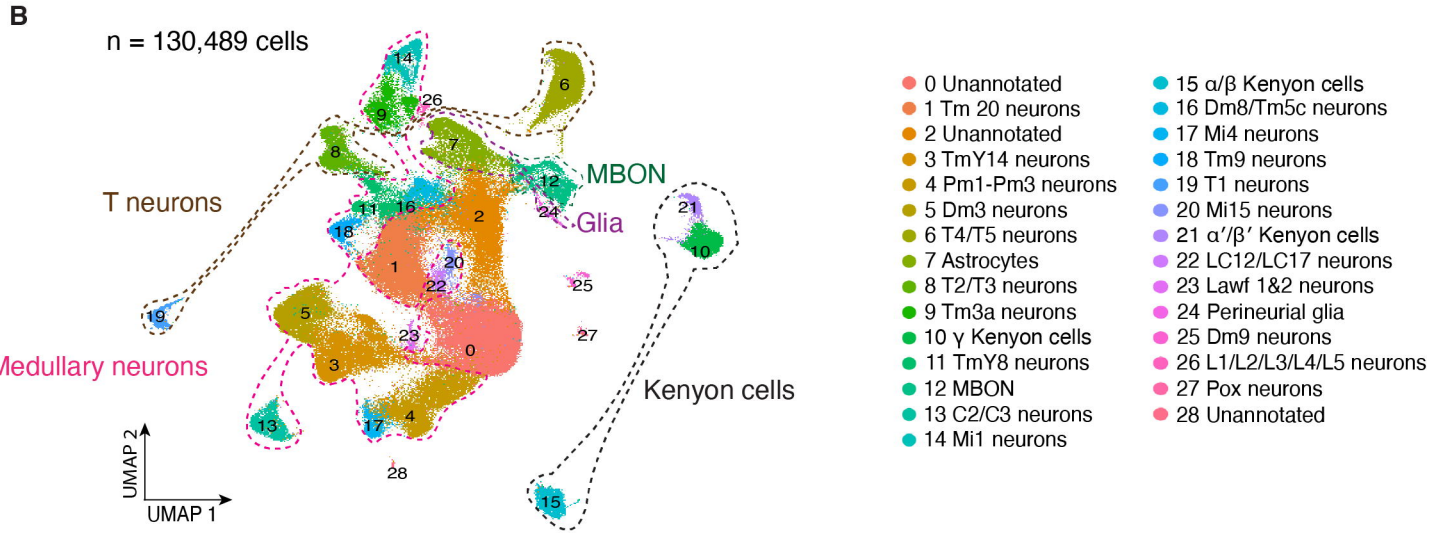
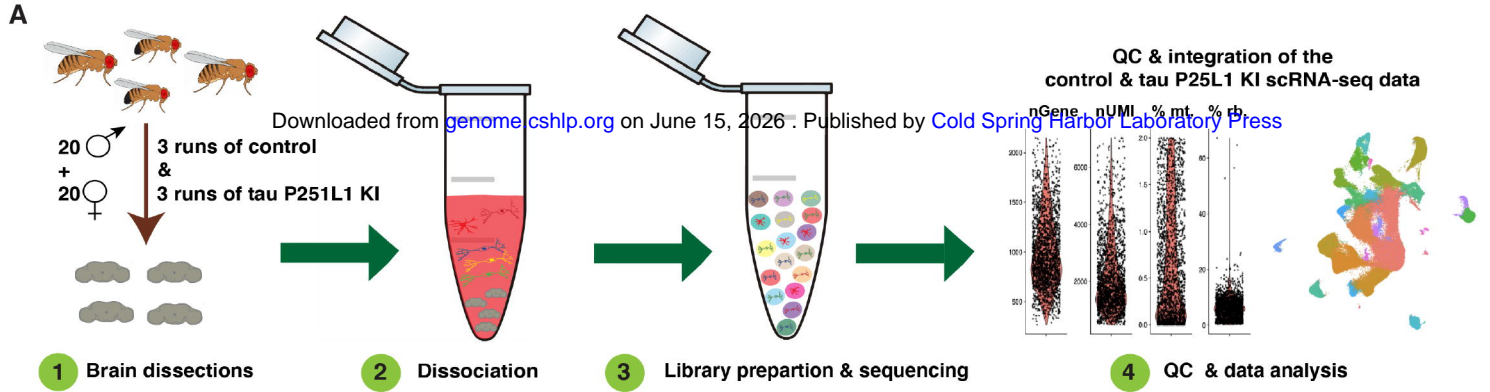
D

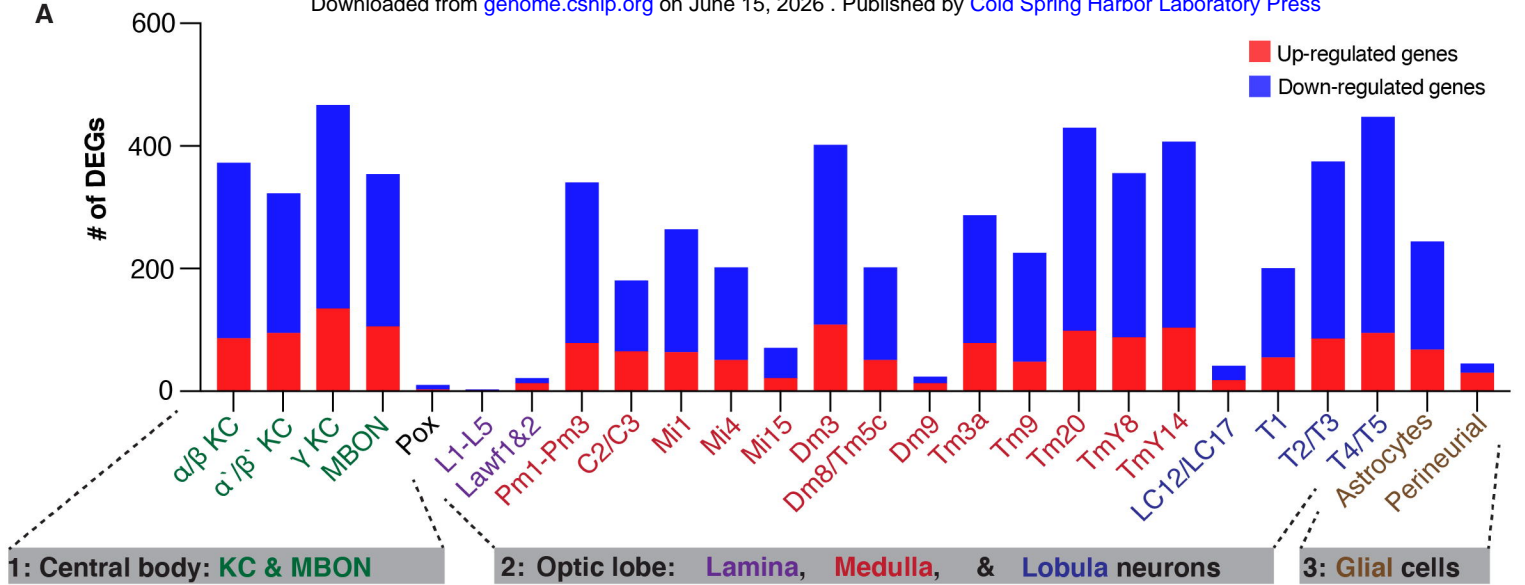


E

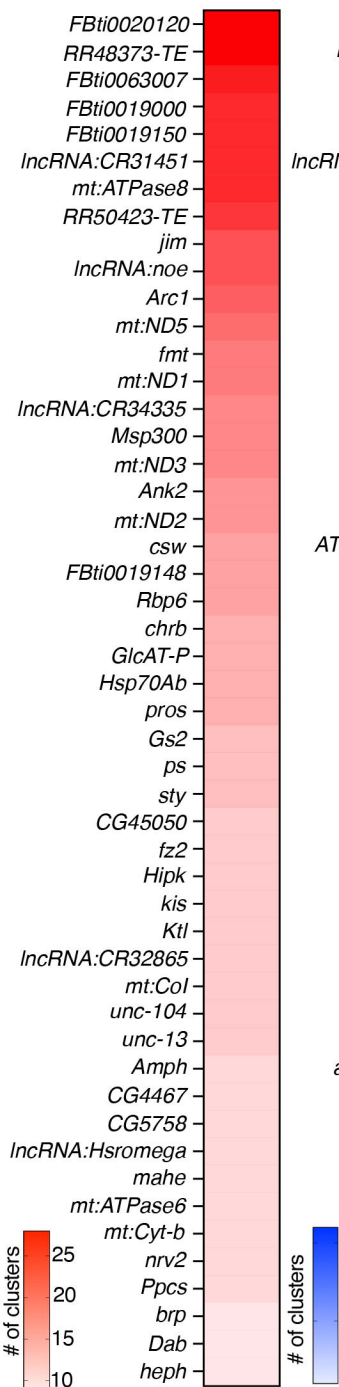




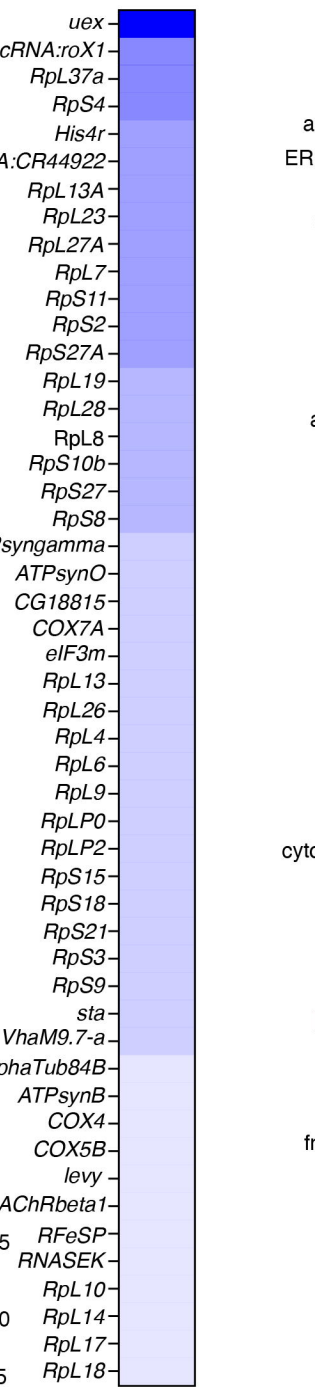




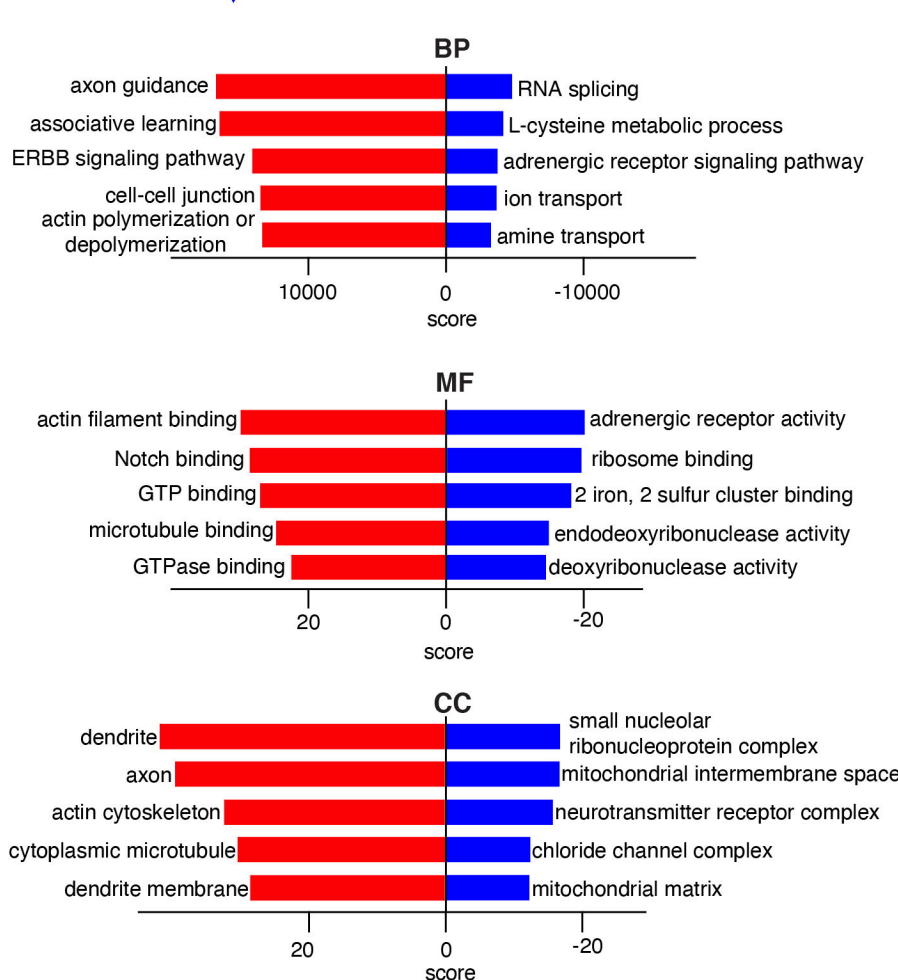
B Up-regulated genes in tau P251L KI brains



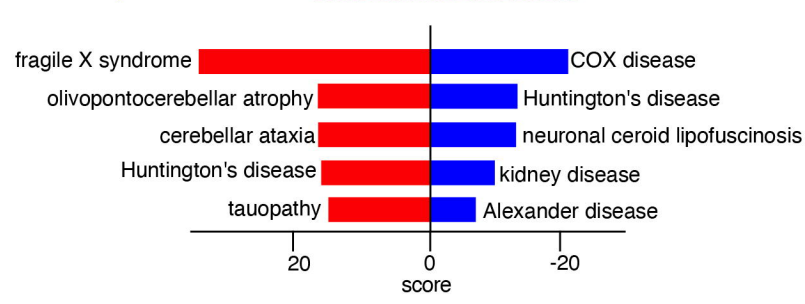
C Down-regulated genes in tau P251L KI brains



D GO terms in tau P251L KI brains



E Genes in tau P251L KI brains associated with human diseases

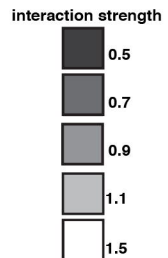
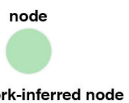
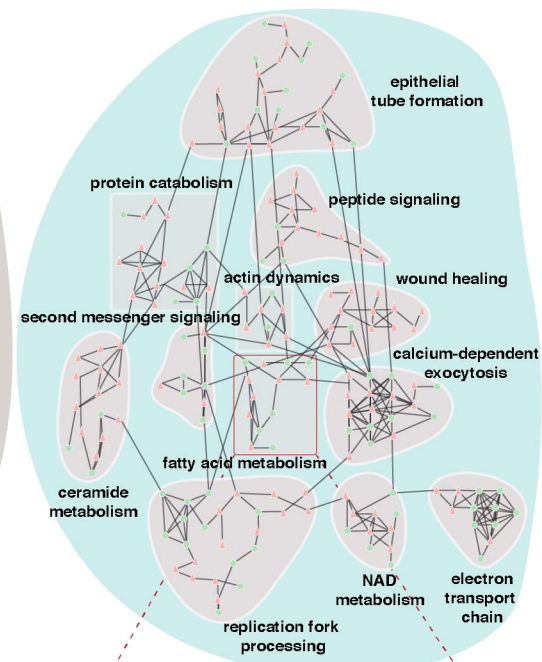
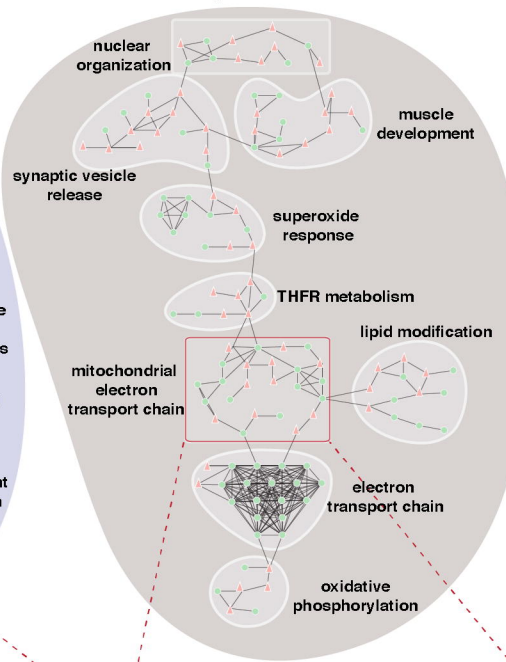
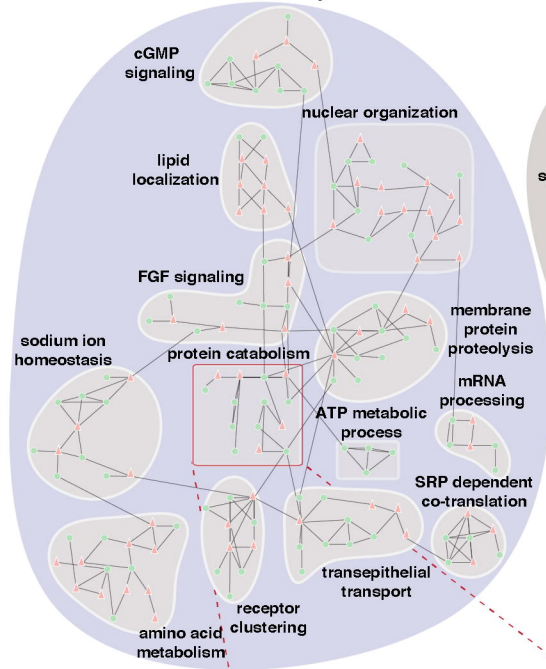


Protein interaction networks enriched in tau P251L KI brains

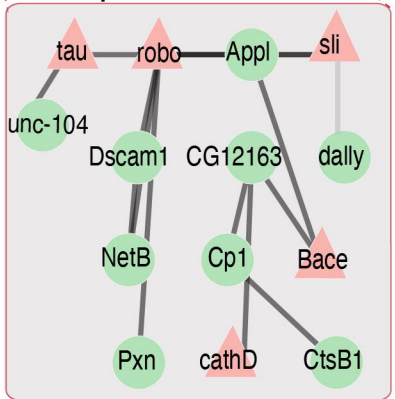
Central Body

Optic lobe

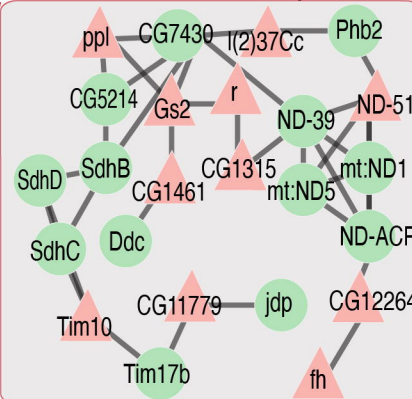
Glia



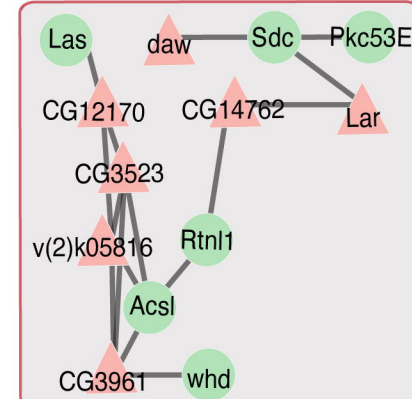
protein catabolism

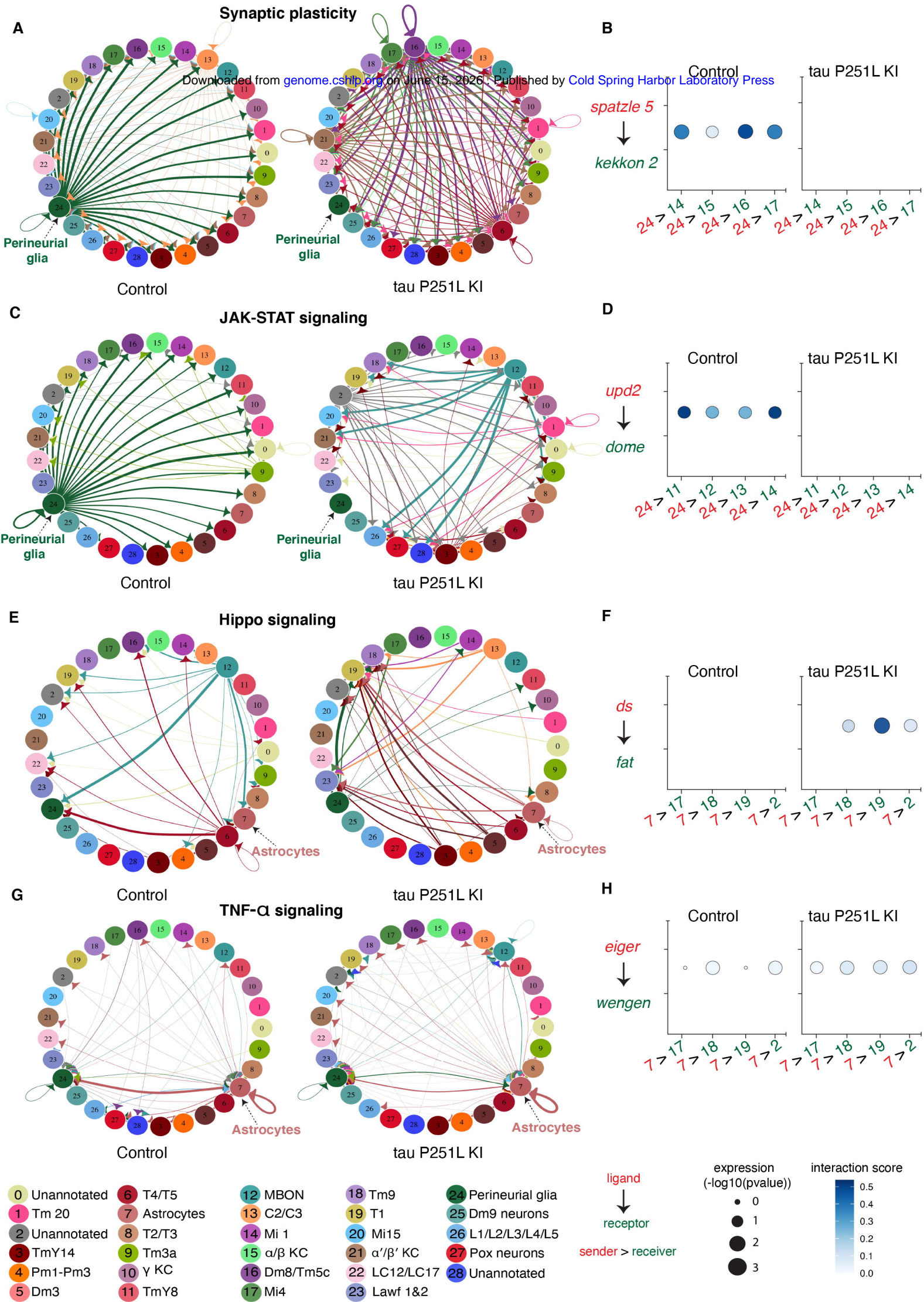


mitochondrial electron transport chain

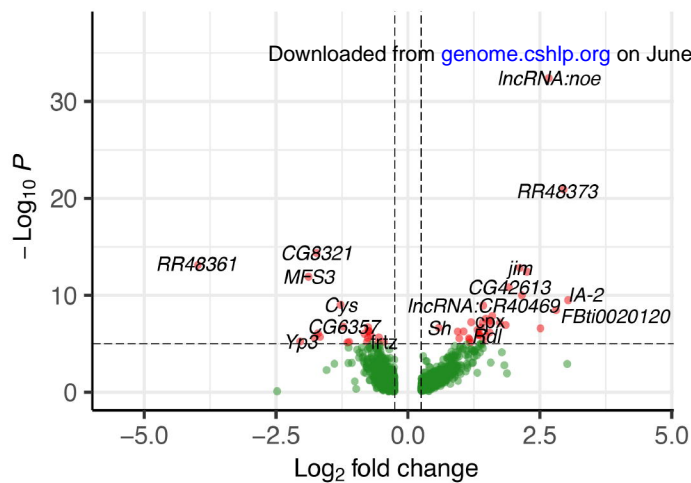


fatty acid metabolism

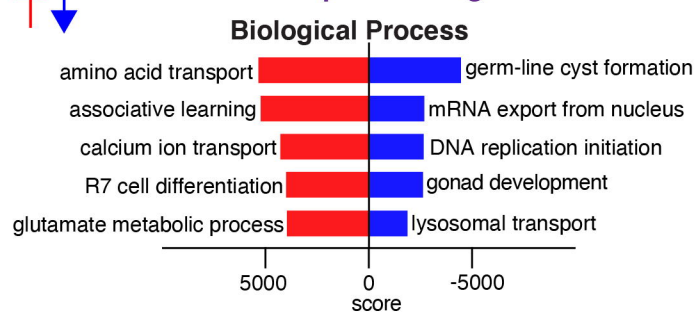




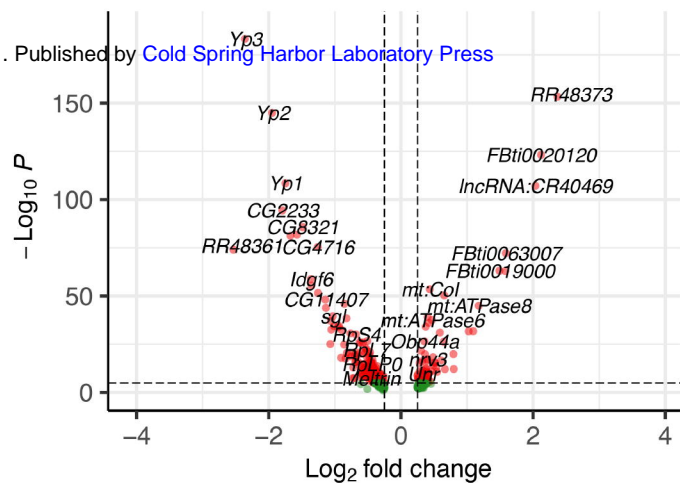
A DEGs in the perineurial glia of tau P251L KI brains



B GO terms in the perineurial glia DEGs



C DEGs in the astrocytes of tau P251L KI brains



D GO terms in the astrocytes DEGs

